RETROFITTING OF INITIALLY DAMAGED BEAM COLUMN JOINT USING CFRP CONFINED UHP-HFRC

A Thesis Report submitted in the partial fulfillment for the award of the degree of

MASTER OF ENGINEERING

IN

STRUCTURAL ENGINEERING

Submitted By

Lovish Goyal

Roll No. 801724013

Under the Supervision of

Dr. Prem Pal Bansal	Dr. Gurbir Kaur	Mr. Raju Sharma
Associate Professor and Head	Assistant Professor	Lecturer
CED, T.I.E.T	CED, T.I.E.T	CED, T.I.E.T

DEPARTMENT OF CIVIL ENGINEERING

THAPAR INSTITUTE OF ENGINEERING AND TECHNOLOGY,

PATIALA- 147004, (INDIA).

JULY, 2019

DECLARATION

I, Lovish Goyal, hereby declare that the work which is presented in this thesis entitled "**RETROFITTING OF INITIALLY DAMAGED BEAM COLUMN JOINT USING CFRP CONFINED UHP-HFRC**" in partial fulfilment of requirements for the award of the Master of Engineering in Structural Engineering, submitted in the Civil Engineering Department, Thapar Institute of Engineering and Technology, Patiala, is an authentic record of the work carried out by me under the guidance of Dr. Prem Pal Banal (Associate Professor and Head CED), Dr. Gurbir Kaur (Assistant Professor), Mr. Raju Sharma (Lecturer) Department of Civil Engineering, Thapar Institute of Engineering and Technology, Patiala.

The matter embodied in this thesis has not been submitted in part or full to any other institute or university for the award of any degree.

Lovish Goyal

Dated: Lovish Goyal

Roll No. 801724013

CERTIFICATE

This is to certify that the above declaration made by the student concerned is correct to the best of my kNowledge and belief.

Dr. Prem Pal Bansal	Dr. Gurbir Kaur	Mr. Raju Sharma
Associate Professor and Head	Assistant Professor	Lecturer
CED, T.I.E.T	CED, T.I.E.T	CED, T.I.E.T
Patiala	Patiala	Patiala

ACKNOWLEDGEMENTS

This thesis work could not have been completed without the help of many people who contributed directly or indirectly through their constructive criticism. It would not be fair on my part if I do not say a word of thanks to all those whose sincere suggestions made this period a real educative, enlightening, pleasurable and memorable one.

First of all, a special debt of gratitude is owed to my supervisor Dr. Prem Pal Banal (Associate Professor and Head CED), Dr. Gurbir Kaur (Assistant Professor), Mr. Raju Sharma (Lecturer) Department of Civil Engineering, Thapar Institute of Engineering and Technology, Patiala for their gracious efforts and keen pursuits, which has remained as a valuable asset for the successful completion of work. Their dynamism and diligent enthusiasm have been highly instrumental in keeping my spirit high. Their flawless and forthright suggestion blended with an innate intelligent application has crowned my task a success.

The cheerful support of my friends and colleagues is sincerely appreciated. Special words of appreciation go to S. Manreet Singh Sidhu, Sh. Hitesh Bhardwaj, Sh. Ram Simran, Sh. Virender Singh and other laboratory colleagues who helped me in my experimental work. I am also thankful to all the staff members of the Civil Engineering Department for their full cooperation and help.

I would also like to thank my family, all faculty, teaching, and non-teaching of Civil Engineering (CED) TU, Patiala for their assistance and my friends for their constant encouragement during the entire period of my thesis work.

LOVISH GOYAL

M.E STRUCTURAL ENGINEERING

ROLL NO 801724013

ABSTRACT

The beam column joint (BCJ) are considered as a vulnerable joint in a framed structure when subjected to cyclic load. The framed structures designed using pre-seismic codal provisions follow the non-ductile approach and the joint was not capable enough to resist the post elastic rotation. The absence of ductility in pre seismic designed reinforced concrete framed structures leads to greater extent of damage in BCJ. With the advent of revised design and detailing codes and increase in the earthquake vulnerability level of many regions, the existing structures need strengthening to conform to the revised codal provision. Therefore, there is a need of retrofitting of BCJ which will significantly improve its performance. The various types of materials used to improve the performance of BCJ e.g. Carbon Fiber Reinforced Polymer, Glass Fiber Reinforced Polymer, steel plates etc. Also, the various techniques such as Jacketing and pre-stressed CFRP has been used to retrofit the BCJ. However, the demerits associates with each technique restrict the performance of retrofitted structure elements. The demerit of jacketing is the increase in size due to encasement consequently the free inside space is reduced. The deb-bonding of CFRP at higher stress resulted in a brittle failure of retrofitted structures/elements. Therefore, it becomes necessary to use such retrofitting technique that can overcome these problems.

Therefore, in the present study CFRP and ultra-high performance hybrid fiber reinforced concrete (UHP-HFRC) were used as retrofitting material for initially damaged BCJ. The development of UHP-HFRC was done by using OPC 53, silica fume, metakoalin, nano silica and steel fibers. The design mix of M20 grade of control specimen was designed according to IS code 10262:2009. The damage index level was calculated with the Park and Ang model to kNow the complete, severe, moderate and slight damage of BCJ. CFRP has been used in the published research as a laminate sheet on the joint but in the present study it was proposed as a CFRP strip mesh form that could be sandwiched between two concrete layers. Retrofitted BCJ was tested under cyclic loading to check the load displacement hysteresis graph. The test results indicated that CFRP confined with UHP-HFRC improves the displacement ductility, stiffness, energy dissipation, moment rotation, joint principle tensile strength and failure pattern of retrofitted specimen as compared to control specimen. The damage index level of BCJ increases, i.e. slightly to completely then ductility, stiffness, energy dissipation, moment rotation, joint principle tensile strength decreases.

CONTENTS

LIST OF TABLES

LIST OF FIGURES

ABBREVIATIONS

CHAPTER - 1

INTRODUCTION

1.1 General

In the various part of world, during the earthquake the reinforced moment resisting structure shows the consequences of the poor performance of reinforced structure. Figure 1.1 shows the typical beam column joint failure. Crucial zones in the reinforced moment resisting structures are load transferring between the beam and column joint. Mostly found that the distress and suffer damage in the reinforced structure even before the service life is over due to several causes, such as overloading, improper construction, earthquakes, corrosion, improper design, flood, fire, wear and tear etc. Mostly found that the small buildings are not structurally designed and they are always made by the experience based contractors. These type of buildings are not earthquake resistant because they were not design according to the codal provisions of the Indian code or any. Due to lack of kNowledge and guidance they always use indigenous techniques. Mostly these type of buildings are affected by earthquake prone areas of developing countries i.e. Turkey, India, Pakistan and japan.

According to Indian design code practice, the design of beam column joint in structure is generally neglected. As per the existing design code, the anchorage reinforcement of the beam concentration is limited in the column which is not an acceptable according to the seismic effect. There have been many severe failures occurred in the past earthquakes i.e. India, Turkey etc. These are occurred due to the wrong/faulty design of beam column joint. There are mainly two types of failure occurred i.e. joint shear failure and anchorage failure.

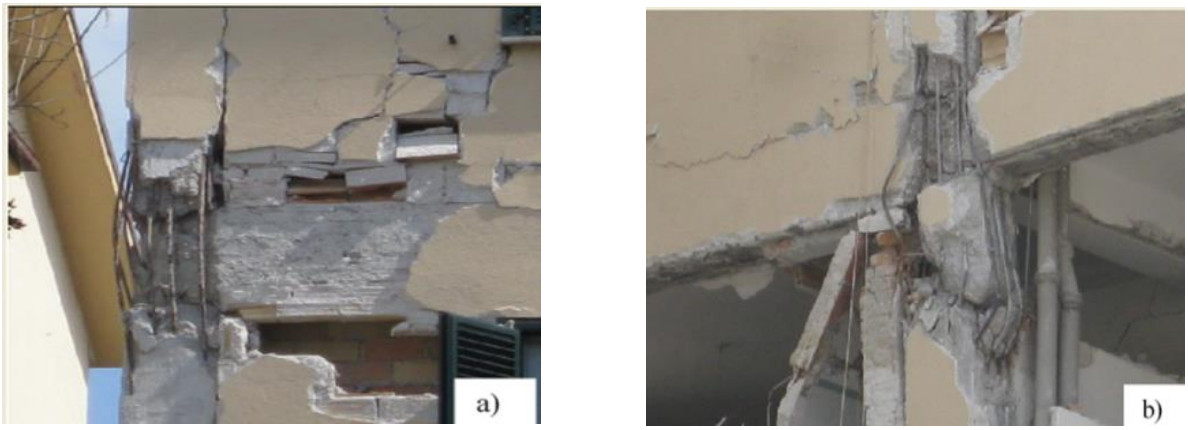

Figure 1. 2 Typical Beam Column Joint Failure (Beschi et al. 2015)

1.2 Building Frame

Building frame is defined as the structure made from the beams and the column. The various types of elements present in the structure are beam, column and beam column joint. There are two type of building frames:-

a) **Rigid frame structure** - A rigid structure are those structures which resist the deformation of structure. Rigid structures are defined as the columns and beams are made monolithically and resist the moments which are generating from the load. These type of structures resist the torsion, shear and moment more effectively than other type of structures.
b) **Braced frame structure** – In braced framed structure, the diagonal members are provided between the columns and beams to resist the lateral forces and side way forces which are applied on the structures and it also increase the efficiency of the structure. Braced frame structure resists the earthquake forces and wind forces more effectively than rigid structures.

In building frame, different types of structural elements are present in the structure like beam, column, beam column joint and foundation. But we are doing work on the beam column joint. In beam column joint various types of joints are present which are discussed in the succeeding section. The various properties like stiffness, ductility ratio, moment graph, energy dissipation etc. are discussed in result section.

1.3 Beam Column Joint

The beam column joint is the crucial zone to make moment resisting frame in a reinforced concrete. Three types of beam column joint can be seen in structure:-

1. Interior joint
2. Exterior joint
3. Corner joint

When an adjacent two sides of vertical face of column are attached with beam, the joint is called corner joint. When all sides of vertical face of column covered with beam, the joint is called interior joint. When three sides of vertical face of column covered with beam, the joint is called exterior joint.

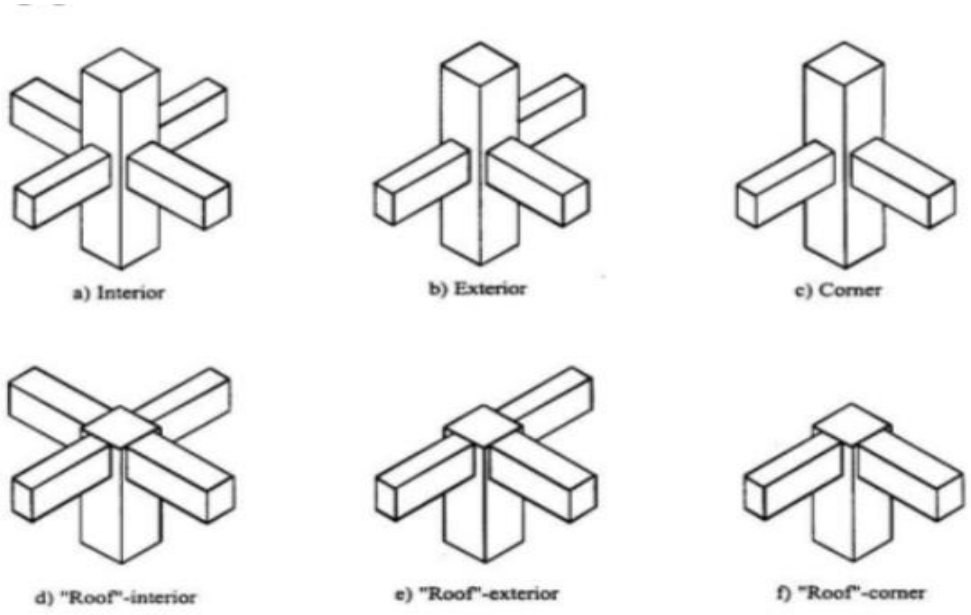

Figure 1. 3 Types of Joints (www.google.com/search?q=types+of+beam+column+joints)

The reinforced beam column joints are the most critical and vulnerable section of the structure i.e. moment resisting structure when it comes under the seismic loads. Mainly seismic design says that the structure which is in the earthquake prone areas they are designed as the weak beam and strong column. The beam column joint act as a brittle then it will show the brittle behavior, the beam column joint as a ductile then it will show the ductile behavior.

Mainly the joints are subjected to large shear stress under the action of the seismic forces. These forces mainly put the stresses on the joint reinforcement. These types of problems have been observed in the past earthquakes in different countries.

Under seismic loading, three phase approach is followed in the framed structure:-

1. The structure must be ductile enough in the case of strong earthquake so that when earthquake will come it will not create more damage to the structure i.e. it must be a repairable.
2. When the moderate earthquake will come, there is some damage to the non-structural elements are permitted, but the whole structure must be stable or to remain in elastic.
3. The structure must have adequate lateral stiffness so that it can control the inter storey drifts which will protect the non-structural elements during minor and frequently occurring earthquakes.

1.4 Behavior of Earthquake Joints

Mostly past and present earthquake tested the vulnerability of reinforced concrete structure by shaking the ground surface. The waves which will impact on the structure are characterized as P wave and S wave. P wave behaves similar to sound waves, when they pass through it they will compress and expand the material. S wave behaves similar to water waves, when they pass through it they will move the material up and down. S waves travel through solids only and P waves travel through solid as well as liquid.

Mostly we kNow that short columns fail more in the seismic region. So, IS code always recommending the long columns in the seismic areas. Long columns helps to reduce the crushing of concrete and diagonal cracking in the joint region or it can also be reduced by providing the shear stirrup bars closely spaced in the joint region. The shear stirrup bars reduce the cracking; resist the shear forces and crushing of concrete.

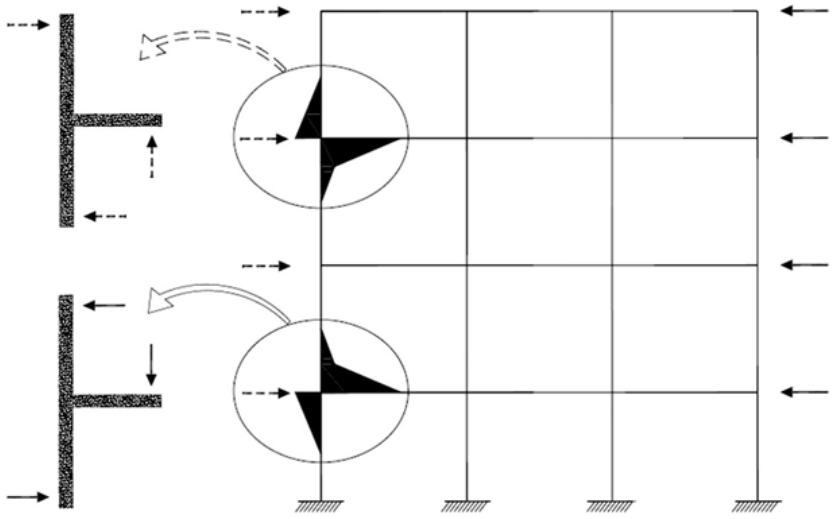

Figure 1. 4 Typical RC Frame (Rajgopal et al. 2015)

When the building comes under the seismic behavior, the lateral forces acting on the structure reduces the efficiency and durability of the structure. During the earthquake, the beams joining with the column develops the moments in anticlockwise or clockwise direction as shown in the figure. The bond stresses developed at the joint i.e. between the steel and concrete try to balance or zero these forces. Mostly beam column are designed as weak beam and strong column. But if this condition is not then frame will sway and failure will takes place. When the structure is in seismic zone and the BCJ are not designed properly means that reinforcement is not according to IS 13920-1993 and concrete is not designed according to IS 10262:2009 then steel will slip inside the concrete, this way the load carrying capacity and

strength will be reduced. Due to seismic effect i.e. push and pull effect, BCJ suffer the geometric distortion at the joint and also increase the elongate and compress the length of BCJ.

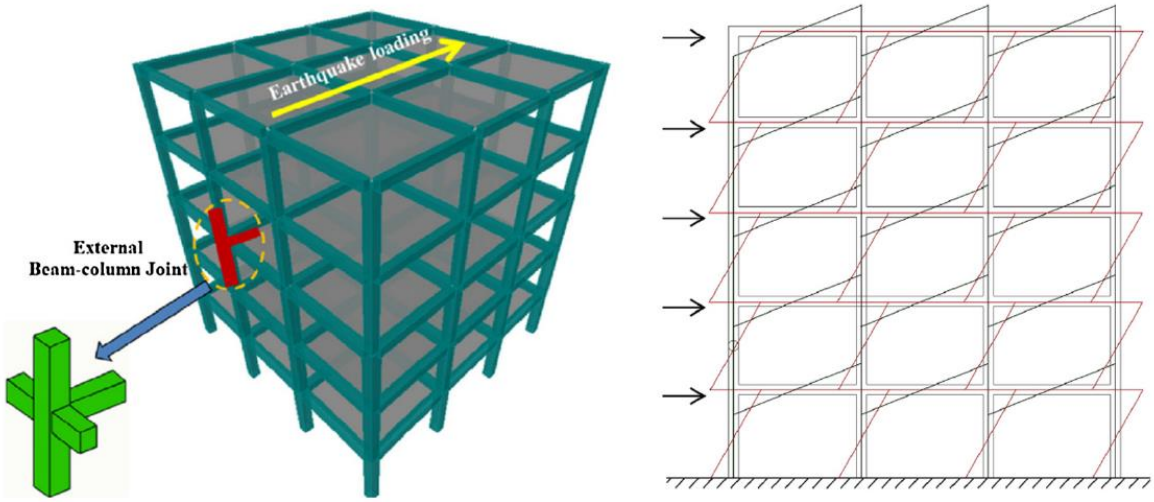

Figure 1. 5 General Arrangement of Building Frame and Moment Diagram Under Seismic Load (Mohammad et al. 2018)

The cross sectional area of the columns is always larger than the beams so that the gripping of bars in the joint will be improved. The structures which lie in the zone 3, 4 and 5 must have min 300mm wide in each direction when the size of columns greater than 4m or the size of span i.e. along beam is greater than 5m according to IS 13920-1993. According to American concrete institute, it recommends the least 20 times the diameter of larger longitudinal bar used. (Senthil et al; 2010)

1.5 Behavior of Beam Column Joints

The basic understanding of beam column joint mechanics tells about the shear transfer within a joint before the retrofitting of the joint. It is also necessary to kNow about the condition of the joint due to seismic forces. The forces acting on the joint depends on the type of load and type of joint. The compression and tension forces transmitted from the beam ends and the axial loads are transmitted by column to the beam column joint.

As earlier seen in the papers, the failure occurs at the joint due to the poor detailing of the reinforcement. Normally in the past they were providing the shear stirrups at larger distance and also not provided the shear stirrups bars at the joint. As earlier, the anchorage bars are not provided at the joint i.e. they were providing the hooks at the joint. That’s why joint will fail

due to the seismic forces. Then some remedial measures could be taken and the stirrup bars provided at less distance and anchorage bars provided at the joint.

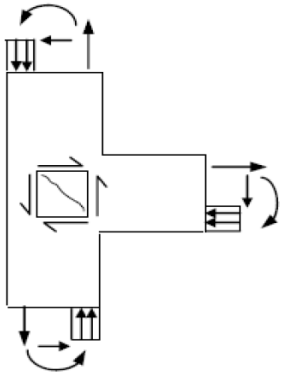

a) Forces

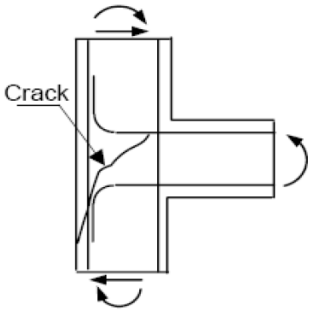

b) Poor Reinforcement Detailing

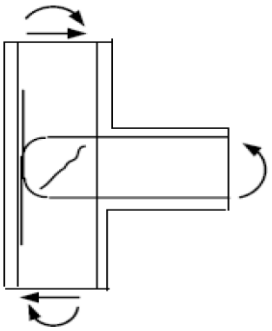

c) Satisfactory Reinforcement Detailing

Figure 1. 6 Exterior Joint

In the exterior column joint, the failure of the joint depends on the detailing of the reinforcement. As the detailing of the joint is poor then the crack will propagate along the column. The cracks are perpendicular to the tension diagonal to the beam column joint and at the faces of beam column joint where the beam ends. As the concrete is weak in tension, therefore provide the reinforcement in the concrete in such a way that it will cross the plane of failure and to resist the diagonal tension forces. The efficiency of the joint depends on the longitudinal reinforcement detailing. The efficiency of the joint depends on the bent up bar provided i.e. if they are provided away from the joint then the efficiency of the joint will be in range of 25-40% and when bent up bars passing from the joint and anchoring them in the joint core then efficiency will be in range of 85-100%.

1.6 Retrofitting

Retrofitting refers to addition of new technology to the older structures. Mostly in India, there are number of structures designed according to older seismic codes. These types of structures are required to maintained or do some modifications according to newer version of seismic codes. Modification of the structures means change in the material properties and structural configuration of the structure. Thus, retrofitting will help to apply various interventions and make the structure earthquake resistant. In general, if the cracks are filled or do some little modification is called repairing, and if we properly change the material at that point i.e. increase the strength level of the structure to pre-defined level is called retrofitting.

Retrofitting of a structure is not same as rehabilitation or repair, whereas the repair means partial improvement in the degraded strengthening of the structure. After the survey of the country, observed that mostly buildings or houses are not made according to the IS code i.e. earthquake resistant. The latest revision of IS Code 1893:2002, many areas of the country come in high seismic zone. So, designed the building or enhance the performance of the structural elements or whole structure there is requirement of retrofitting techniques. The main objective of retrofitting according to IS Code 13935:1935 is -

- To increase the stiffness of the structure.
- To increase the load carrying capacity of the structure.
- To remove the impotent points, where stress consideration is possible.
- To improve the energy absorption capacity and energy dissipation.

1.6.1 Retrofitting steps

a) Assessment

In the assessment, collect the data related to the structure which is required for the evaluation process, preparation of drawings at site, drawings according to the newer version of code (if applicable). If a building fails then check how it will reach to its same level by using different codes. Check the capacity ratio of the structure i.e. if it is less than 1 then retrofitting is essential.

b) Retrofit Scheme

Retrofitting of the structure depends upon the size, deficiency of the structure and importance of the structure. Also check that which member of the structure to be strengthened. The various retrofitting schemes are discussed in other sections.

c) Selection of Retrofitting Scheme

In this section, firstly study about the failure pattern of the structure. Then select the suitable type of retrofit scheme for the structural member.

d) Construction and Monitoring

Firstly check whether selected retrofit technique is executable at site or not. Check any deficiency in the retrofit technique at the time of execution. This way we can change the strategy if it is not suitable.

1.5.2 Retrofitting plan

Retrofitting Plan can be classified into two categories:-

1. Global Retrofitting
2. Local Retrofitting

a) Global Retrofitting

If whole structure is retrofitted and fulfills the serviceability requirement of the structure, this retrofit refers to global retrofit. In this entire structure is designed according to the specifications of IS codes.

Global Retrofitting involves processes like

1. Adding shear wall
2. Adding infill walls
3. Adding bracings
4. Wall thickening

b) Local Retrofitting

In this only specific member of the structures are retrofitted i.e. some structural elements of building.

Local retrofitting involves

1. Jacketing of columns
2. Jacketing of beams
3. Jacketing of beam column joint

1.6.3 Retrofitting techniques

There are various repair techniques as discussed below:-

a) Mortar Injection Technique

Mostly this type of technique is used to repair of older works. It is used where the introduction of concrete is difficult in the cracks of the structure. In this technique, pre-mixed mortar is used. Firstly grout the crack to some extent so that mortar injection can takes place.

b) Epoxy Injection Technique

It is used for the repairing of fine cracks and surface coating. It depends upon the viscosity of material. It is used to enhance the performance of the structure by filling the voids and rebinding the cracks.

c) Shortcreting Technique

This technique is suitable when the cracks are in large number and the size of cracks is larger. In this technique, the concrete mix is sprayed in-situ is called shortcreting.

d) Epoxy Mortar Filling Technique

In this technique, mixing of epoxy of high or low viscosity with the concrete and applied on the cracks where the concrete has lower compressive strength, tensile strength and higher elastic modulus than epoxy.

e) Repair and Replacement Technique

Repair the broken point of the structure if the damage level of the broken is not upto moderate level than replace the material of that point.

f) Plate Bonding Technique

The plate bonding technique depends on the compressive and tensile strength of material. As the concrete is having lower tensile and higher compressive strength. In order to increase the strength of concrete plates by using special material i.e. fibers so that web faces of the structures enhance their efficiency.

Mostly these types of plates are commonly used these days:-

I. Ferro-cement Plates
II. Fiber Reinforced Polymer (FRP) Plates
III. Polymer modified concrete and mortar PMC/PMM

IV. Steel plates

The salient features of each of these techniques are:-

a. Ferrocement Plates

Ferro-cement refers to the small size wire mesh of equal size boxes. This ferrocement layer is sandwiched between the two concrete or mortar layer. This ferrocement helps to resist the shear, impact, fatigue stresses and high tensile stresses with outstanding maintenance to corrosion. The ferrocement plates increase the load carrying capacity of BCJ by casting in-situ or using the adhesive material on the chipped surface of BCJ. Ferrocement has less cost as compared to other materials.

b. Fiber Reinforced Polymer (FRP) Plates

A group of materials collected with organic and inorganic fibers implanted in a resin matrix is called as Fiber Reinforced Polymers. FRP material has high tensile strength and stiffness. They are resistance to corrosion, non-magnetic material, light in weight which will help to make the material appropriate for the retrofitting and strengthening of the joint. The main advantage of FRP is high corrosion resistance and high strength to weight ratio. Some examples of FRP are carbon fiber reinforced plastic, glass fiber reinforced polymer etc. are used in the industries. The sheets of FRP are very thin, flexible and easily fit in the material.

The drawback of FRP is that it loses its properties at high temperature.

c. Polymer Modified Concrete and Mortar PMC/PMM

The grouping of single polymer in mortar or concrete is called polymer modified concrete. They are mixed during the preparation of material. The particles of polymer are very small in diameter that it can emulsify with water. They are also used in dispersible powder form when preparation of dry cement aggregate is there. It will reduce the permeability but increase the workability of concrete. The main advantage of PMC is that it increases the adhesive and binding properties of cement concrete.

d. Steel Plates

This retrofitting technique is mostly used where the reinforcement is missing or the crack width increases. This steel plate retrofitting technique helps not to increase the crack width of joint. Steel Plates provides the stiffness, ductility, strength and stability to structural elements. Through steel plates higher flexural strength and stiffness can be achieved in tension plats. There are two type steel plates i.e. U-shaped and L-shaped steel plates. These steel plates provided on the side faces of structural elements or on the tension side.

1.7 Gap and Objective of Work

1.7.1 Gap in the research area

The main aim of research is to develop the UHP-HFRC and to strengthen the BCJ by retrofitting using CFRP confined with UHP-HFRC. But the investigation on the development of UHP-HFRC is rare and the application of UHP-HFRC at the site is not in common use. Also the curing temperature of UHP-HFRC is ambient which restricts as a factory controlled material.

The CFRP used in the research improves the behavior of BCJ. Earlier the CFRP used as a laminate at the bonds like wrapping along the beam and column, L shaped cutting, diagonally bonding at the joint. There is no research on the configuration of sandwiched form of CFRP i.e. CFRP placed between two layers. Aim of study to reduce the use of CFRP and make them economical. In our research, CFRP strips used to make a strip mesh at the joint with the help of epoxy. It is difficult to form strip mesh at the site but it increases the strength of BCJ. To give concise literature review on the development of UHP-HFRC and the retrofitting of BCJ with CFRP confined with UHP-HFRC is also aimed at in this report.

1.7.2 Objective of the research work

Keeping in view the gap in research area, the objectives of the research are as follows:-

1. To develop the UHP-HFRC.
2. Devising a new retrofitting scheme using CFRP strips and UHP-HFRC to analyze in terms of ductility, stiffness, energy dissipation, moment rotation , principle joint tensile stress and failure pattern of retrofitted beam column joint under seismic load.

CHAPTER 2

LITERATURE REVIEW

2.1 General

Mostly seen that thousands of the structures are constructed day by day, larger number of structures deteriorates before the design life of the structure. The reasons behind this problem due to unexpected loading conditions, improper design, supervision problem, codal provisions and faulty construction etc. This structure requires immediate attention so that some remedial measures can be taken and brings it back to its functional use again. To overcome this problems various type of retrofitting techniques are used like ferrocement, CFRP, GFRP or by some other materials like UHP-HFRC, HPHFRC etc. In published papers, CFRP and GFRP laminates used at the BCJ for retrofitting process. It is observed in the published papers, there is debonding of CFRP takes place at the BCJ. Reinforced material is one of the most important construction material used in the developed and developing countries. Concrete is a brittle material, has higher compressive strength and lower tensile strength. It is also heterogeneous in nature. To develop the UHP-HFRC or HP-HFRC, the mix contains steel fibers, silica fume, metakoalin, fly ash, GGBS etc. These ingredients increase the compressive strength, flexural strength, workability etc. The steel fibers improve the tensile strength of concrete. The steel fibers resist the growth of crack or delay the propagation of cracks whereas binder content fill the pores of concrete.

2.2 Retrofitting of Beam Column Joint

Raju et al. (2019) studied the behavior of BCJ by retrofitting with UHPC. The four damage levels are calculated i.e. completely damage (CD), severe damage (SED), moderate damage (MD) and slightly damage (SD). These specimens are designated as C-CD (control specimen) and retrofitted specimens are R-CD, R-SED, R-MD and R-SD. The size of specimen i.e. beam cross sectional area is 225mm*125mm and length is 950mm, column cross sectional area is 225mm*125mm and column length is 1000mm.

The experimental result showed that the C-CD specimen when strengthened with the UHP-HFRC then it becomes R-CD. The testing of R-CD specimen under cyclic load there is 103% increase in the load value as compared to C-CD on tension side and on compression side it is same. This indicates that there is improvement at the joint and also achieved the same capacity as control level. As the damage level increase i.e. slightly to complete damage therefore the

ductility of the retrofitted BCJ decreases from 45.29% to 20%. The cumulative energy dissipation of retrofitted specimen increases as the damage level decreases i.e. 3588 kN-mm to 8894 kN-mm. The slightly damage BCJ after retrofitting, the ultimate failure point of R-SD exceed the control specimen i.e. 35 to 45mm. The peak to peak stiffness of BCJ increases as the damage level of BCJ decreases. The sequence of retrofitted specimen in terms of peak to peak stiffness is R-SD>R-MD>R-SED>R-CD.

Ibrahim et al. (2018) studied the retrofitting of BCJ with the ferrocement layer to check the stiffness and strength of BCJ. They have made the total eleven specimens in which one specimen detailed according to traditional practice, second according to ACI 318 and other nine specimen in which orientation of ferrocement present i.e. 45^o and 60^o and variation in number of layers of ferrocement at the joint.

The experimental result shows that the joints which are retrofitted with the ferrocement layer shows the higher ultimate displacement, higher load carrying capacity and shows the better ductility. They did not show the heavily damage at the joint during testing. As the number of ferrocement layer increases, the ultimate load carrying capacity of the BCJ and ultimate displacement increases. It is also observed that the strength of specimen whose orientation angle is 60^o show the better result than 45^o because the orientation of 60^o wire mesh is perpendicular to the crack and resist the crack on the BCJ. The specimens which were retrofitted with the steel angles and ferrocement increases the seismic performance, also there is stability in strength degradation and achieves higher capacity of energy dissipation.

Mohammad et al. (2018) studied the seismic performance of BCJ retrofitted with HPFRC. The six specimens were developed in which various types of reinforcement present i.e. ductile and non-ductile reinforcement in the BCJ. The figure 2.3 – 2.5 depicts about the types of concreting in which there is no HPFRC (NC), HPFRC present at the joint but in T shape, denoted as C2-HPFRC and other HPFRC present in the BCJ but only in beam, denoted as C1-HPFRC.

The experimental result show that the maximum load carrying capacity increases by 24.15% and 8.45% as compared to normal concrete with ductile and non-ductile respectively. The ductility factor in HPFRC BCJ with seismic detailing in negative and positive directions is increased by 31.33% and 12.43% as compared to control specimen of ductile and non-ductile detailing respectively. The cumulative energy dissipation of HPHRC BCJ at the drift 6% is 3.45 and 1.33times the non-ductile and ductile detailing respectively.

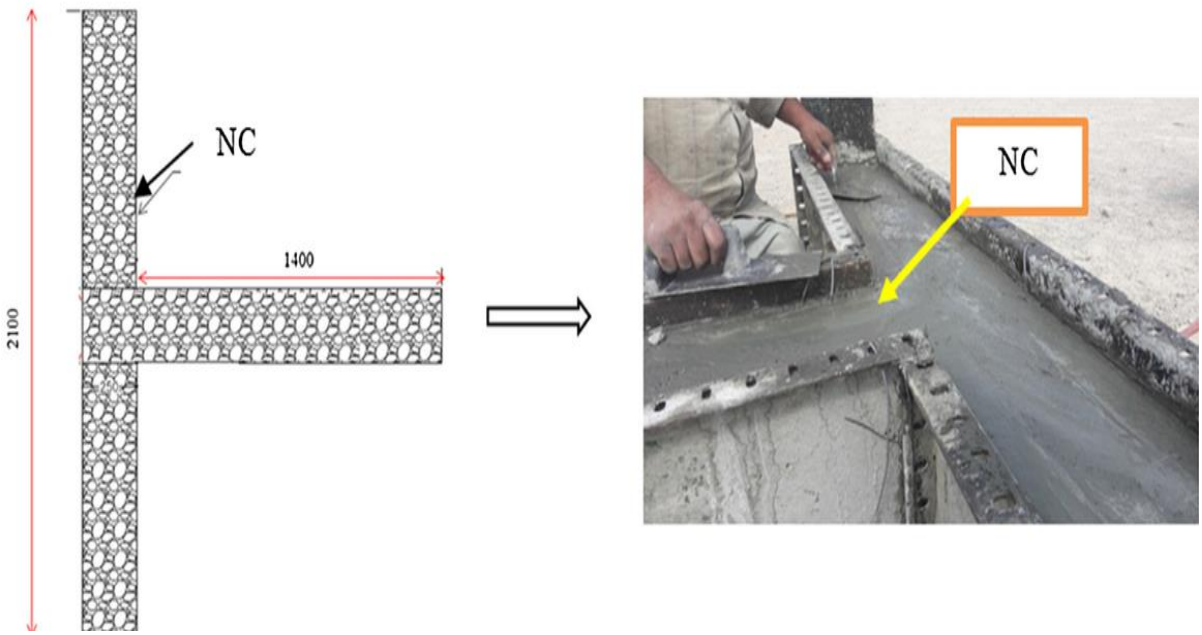

Figure 2. 1 Concreting Pattern for C1 (Mohammad et al. (2018)

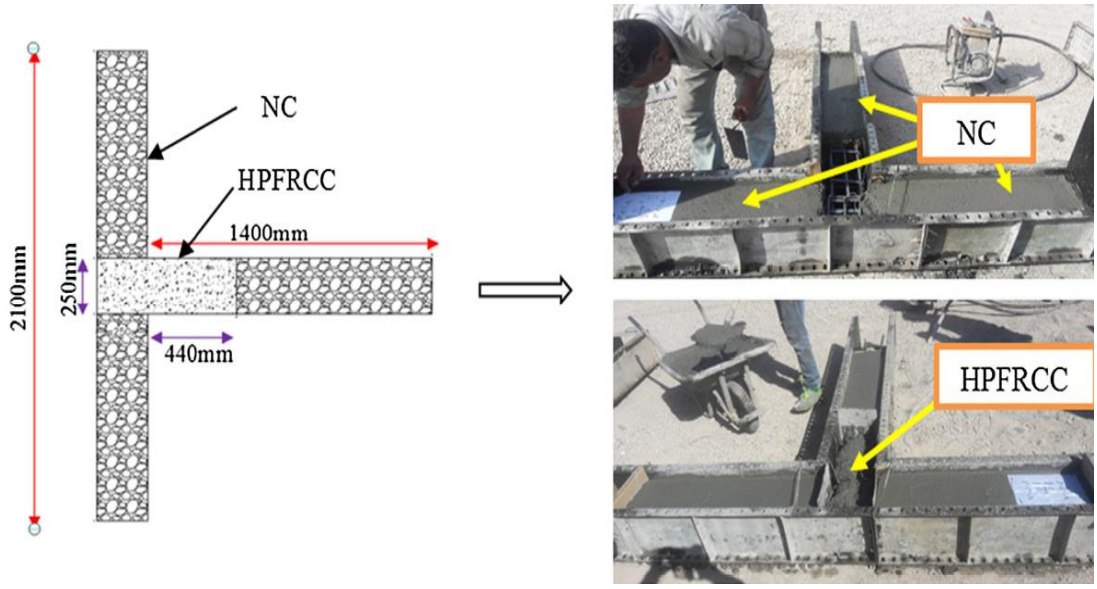

Figure 2. 2 Concreting Pattern for C2 (Mohammad et al. (2018)

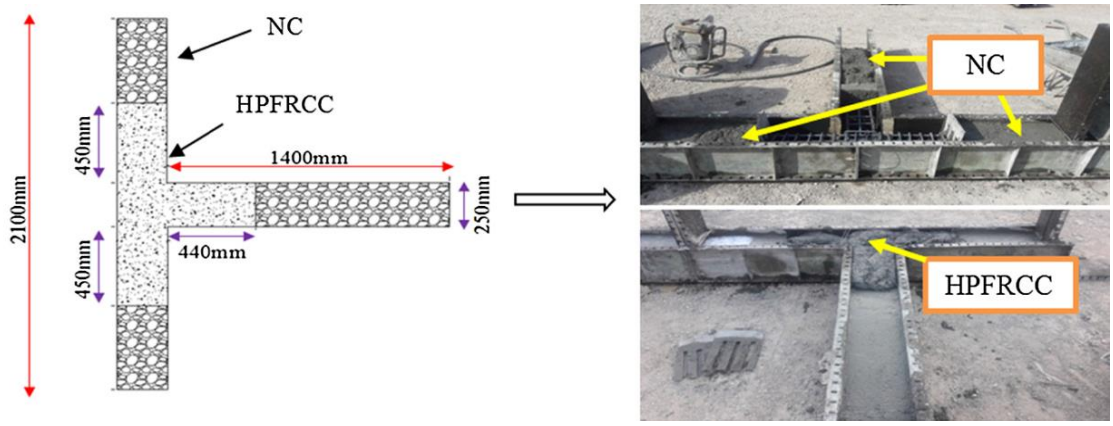

Figure 2. 3 Concreting Pattern for C3 (Mohammad et al. (2018)

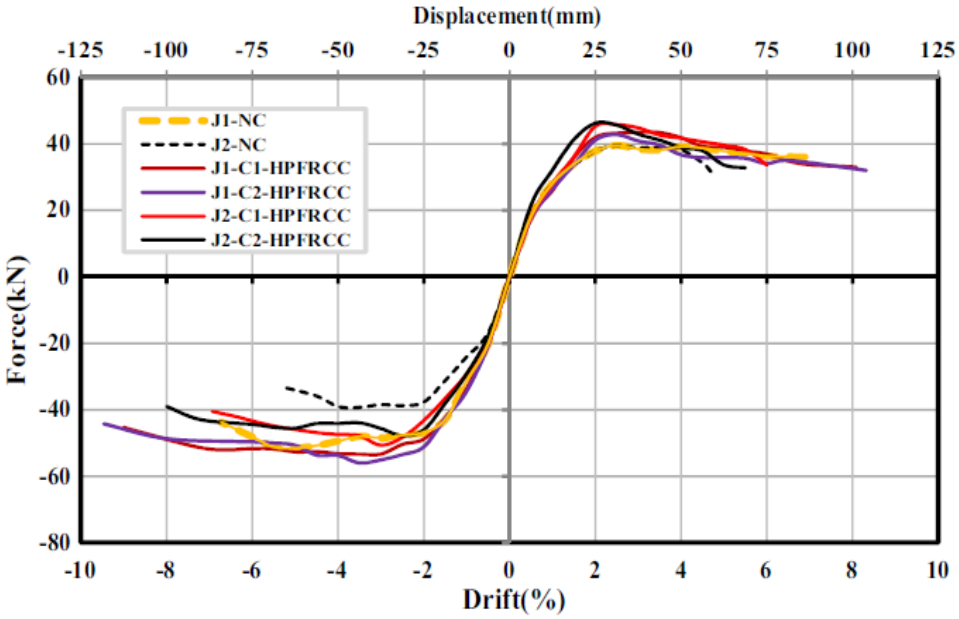

Figure 2. 4 Load Displacement Envelope of Specimens (Mohammad et al. (2018)

Bansal et al. (2016) studied the retrofitting of BCJ with ferrocement. In his study, five specimens were made in which one of them control specimen (CS), other four are made up of two retrofitting schemes i.e. in RS-I, wire mesh is provided in L shaped at bottom and top of the BCJ and on other side RS-II, wire mesh is provided same as RS-I but provided the diagonally to the joint also. The retrofitted specimens are loaded with 80% of the ultimate load. The figure 2.7 shows specimen retrofitted with both schemes (RS-II AND RS-II).

Figure 2. 5 Specimen Retrofitted with Mesh Wire (Scheme I and Scheme II) (Bansal et al., 2016).

The experimental results show that the ultimate load carrying capacity of the retrofitted specimen increases with ferrocement i.e. for R-1 specimen load increases from 55 kN to 81.45

kN, for RS-II specimens load increases from 55 kN to 81.52 kN. However, when compared the ductility of retrofitted specimen with control specimen it shows that the value decreases. The value of energy absorption of RS-I decreases by 8% and the RS-II decreases by 4% as compared to the control specimen.

Singh.V et al. (2014) studied the behavior of BCJ and strengthening with the CFRP jacketing.. The sizes of specimen i.e. beam and column cross sectional area is 225mm*125mm and length of beam and column is 500mm, 1000mm respectively. The figure 2.8 presents the retrofitting of BCJ with CFRP.

Figure 2. 6 Retrofitting with CFRP (Singh.V et al. 2014)

The total nine numbers of specimens are made for the testing purpose the jacket provided on the BCJ is in L shaped and orientation is 45^{o} to the joint in two layers. Three Specimens are tested as control, remaining six i.e. two are tested upto ultimate load, next two are tested upto 85% of ultimate load and next two are 50% of ultimate load.

The retrofitted specimen shows the increase in the load carrying capacity of BCJ is 7 to 12% as compared to the control specimen. There is increase in the yield load of retrofitted specimen is 15% as compared to control specimen. The stiffness of the specimen which are stress level at 2 and 3 having 17.36% and 26.94% more than the specimen which is stressed at level 1 because the decrease in initial stress level from 100% to 85% and 50%. The failure point of BCJ transfers from column to beam which will prevent from collapse of structure.

Lee et al. (2010) studied the retrofitting of BCJ with CFRP. The total three number of interior BCJ were casted in which two are strengthened with CFRP and one prototype specimen for the testing purpose. The size of beam and column is 300mm*600mm and 400mm*400mm. The name of the specimens are JI0, JI1, JI2 in which JI0 is the prototype and JI1, JI2 are retrofitted specimens. In JI0, the four unidirectional CFRP was placed at corners at a distance of 50mm; in JI1 specimen, CFRP was placed at corners and also wrapped the CFRP horizontally around the column; in JI2 specimen, CFRP placed four unidirectional applied to the joint zone along the column for a distance of 300mm and similarly along the beam for a distance of 300mm. The four steel angles are applied on the specimen shown in figure 2.9. There is de-bonding of the CFRP laminate takes place, so to avoid de-bonding at the joint anchorage was used in JI2, not in the JI1. The JI1 and JI2 specimen figure given below:-

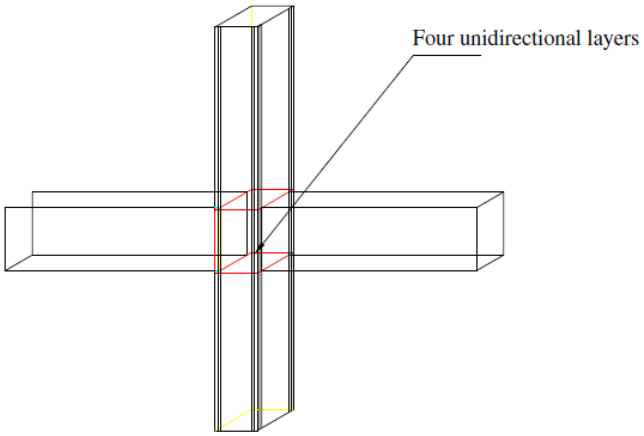

a)

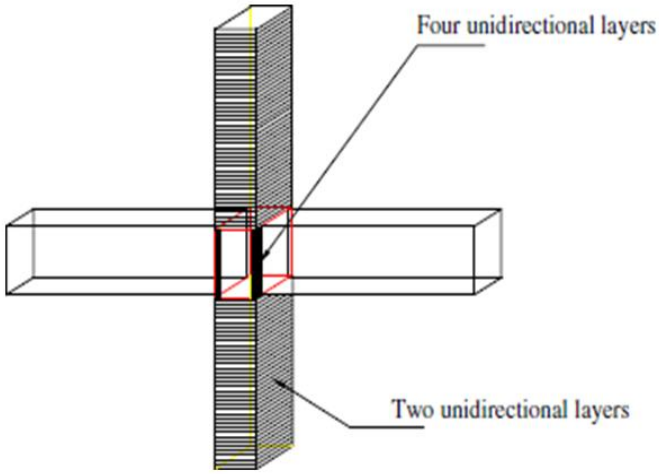

b)

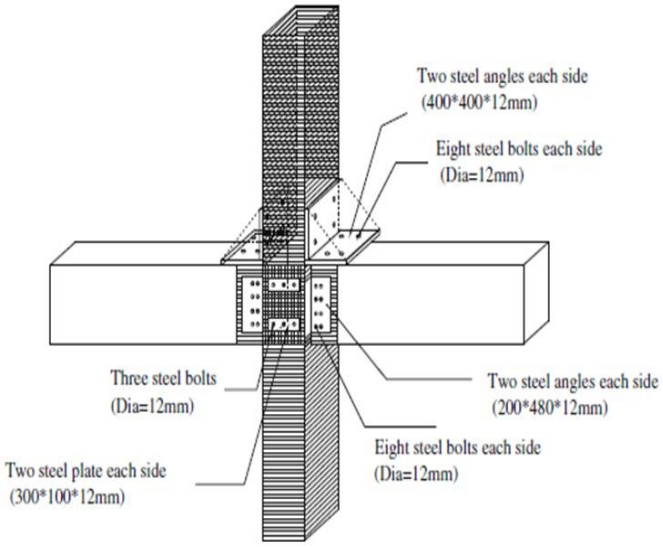

c)

Figure 2. 7 a) Four Unidirectional CFRP at Corners of BCJ at a distance of 50mm, b) Four Unidirectional Layer at Corner and Horizontal Layer along the Ccolumn, c) Rehabilitation Scheme for Specimen JI1and JI2 (Lee et al. (2010))

The experimental result shows that there is increase in strength of JI1 is 4% of specimen JI0 which is almost same as control specimen. The ultimate load carrying capacity of JI2 is 36% of the control specimen JI0. The energy dissipation of JI2 is 90% higher than JI0 it shows that rehabilitation scheme enhances the strength of JI0. As the beams are strengthened with CFRP, can decrease the normal strains. The CFRP strengthened beams shows the lower rate of stiffness degradation especially in JI2.

Sharma et al. (2010) studied the behavior of BCJ retrofitting with CFRP and GFRP. The structure was tested under pushover load in which BCJ pushes till it reaches to its failure point and then retrofitted with the combination of CFRP and GFRP. The retrofitted specimens are tested under the same loading condition as done in case of control beam. The experiment results show that the structure would not able to reach the original stiffness as compared to control specimen and also not able to achieve the 95% base shear as compared to the control specimen due to unevenness of the surface there is de-bonding takes place. Laminates will prevent the spalling of the concrete, and it will improve the joint behavior but the ultimate failure will take place.

2.3 Development of UHP-HFRC

In section 2.3, a literature study on the various mix design models for UHP-HFRC has been discussed. The effect of hybrid fiber system and binders has been discussed on freshly and hardened properties of UHP-HFRC. The high carbon dioxide emission, energy consumption and high cost of raw materials for the production of UHPFRC resist the major application. Hence, in my research work, efforts have been done to attenuate both its environmental impact and economic. The industrial byproducts used in the research work like metakoalin, silica fume etc., as pozzolanic materials, hybridization of fibers and design methodologies used for optimum particle packing of different materials to optimize its use are some of work to achieve the above objectives. In this freshly properties of the UHP-HFRC are discussed in the succeeding section like workability, compressive strength and flexural strength.

2.3.1 Workability

Workability is an important factor for the production of UHPC. As we know that concrete is brittle in nature, with the addition of fibers it imparts some ductility to the concrete. Fibers must be uniform in the concrete to make them concrete reliable and consistent. As the fibers content increases in the concrete decreases the workability of concrete due to the interlocking of the fibers. It is observed that UHPC concrete used in the prestressed structures i.e. bridges or slender architectural shapes etc. So, it requires the workability of concrete will be less aggressive because it creates difficulty in placing of concrete.

a) Effect of Binder Material

Binder material like metakoalin, silica fume, GGBS and fly ash enhancing the freshly properties and mechanical properties of concrete. The workability depends upon the size and shape of binder material.

Yu Su et al. (2017) studied the effect of silica fume, silica flour, Nano Al_2O_3 and Nano TiO_2. As the silica fume is used as a reactive material i.e. involving in the hydration process of cement. Silica flour was used to fill the pores between the aggregate and cement paste. As Nano material and silica flour will have high surface area and the outcome of material will decrease in workability.

Kou et al. (2011) studied the workability of concrete contains the metakoalin, fly ash, silica fume and GGBS on the properties of natural aggregate concrete. The presence of the finer material in the concrete means the higher surface areas of metakoalin and silica fume as compared to cement particles. The specific surface area of material increases the workability

of concrete decreases. The replacement of cement with GGBS and fly ash increases the workability of concrete. The shape of fly ash is spherical which increases the workability of concrete.

Mazloom et al. (2004) examined the effect of silica fume on the workability of high strength concrete. The replacement of cement with silica fume is 0%, 6%, 10%, and 15%. The test results show that as the content of silica fume increase, the workability of concrete decreases because the size of silica fume is much smaller than the cement and as the size is small therefore the high specific area available which blocks the path of free water for workability.

a) Effect of Hybrid Fiber System

Hybrid fiber is defined as the mixture of two different fibers of different material, size or shape in the concrete. Different fibers have different properties and it will become effective and economical when they are used both together then workability of concrete increase because by volume long fibers will become less in quantity and mixing will take place easily.

Raju et al. (2019) showed the method to development of UHPC by using the binder and fibers in the mortar. To increase the strength of concrete, used the binder material like silica fume and metakoalin in the mortar as a filler material and also used the short crimped fiber and long straight fiber in the material. The aspect ratio of short crimped fibers is 25 and long hooked fiber is 80. As the single fiber used in the material could not mix with ingredients easily and the quantity of fiber will decrease if we will put the fiber in the hybrid form and mixing take place easily.

Yu Su et al. (2017) studied the effect of waved steel fiber, short straight fibers and twisted fibers. The aspect ratio of twisted fiber, waved steel fiber, short steel fiber 6mm length and 12mm length are 87.5, 60 , 50 and 100. The quantity of steel fibers was varied from 1-2.5%. The various types of fibers used in the mixture due to which mixing of fiber take place easily because single fiber will interlock with each other and reduces the workability. Therefore the workability of concrete increases by hybrid fiber system.

Yu et al. (2015) showed the method to develop the UHPC by using the fibers and binder material according to Modified Andreasen and Andreasen particle packing model. Nano silica is in liquid form used as a pozzolanic material. To make the sustainable concrete, limestone powder was used as replacement material in the cement. Micro sand whose size is 0 to 1mm and normal sand is used. Binder content in the concrete is 620 kg/m^3 used which is very less

as we design the UHPC. The aspect ratio of hooked fiber, short straight fiber, long straight fiber is 64, 37.5 and 65 respectively.

The effect of single and hybrid fiber on the flow ability of the mix of concrete. It is cleared that as single and short straight fiber is used then the slump value increases firstly then suddenly decreases. The use of hybrid fiber i.e. long hooked and straight fiber in the UHP-HFRC increases the slump value upto 88.5cm.

2.3.2 Compressive strength

This section discusses the compressive strength of concrete. There are many materials used in concrete to perform well in compression like OPC 53 grade cement, coarse aggregate, lower water cement ratio leads to the high compressive strength of concrete. The ingredients used in the UHP-HFRC as a binder materials like silica fume, metakoalin, GGBS, limestone powder, quartz etc. on the other hand hybrid fibers are used in the UHP-HFRC will help to increase in compressive strength.

b) Effect of Binder Material

Raju et al. (2019) studied the various mixes in which changing the proportions of cement, silica fume, metakoalin at standard water curing at 27^{o}C. With the increase of silica fume upto 15% and metakoalin upto 10%, the compressive strength increases day by day. As the water binder ratio decreases in each trial also increases the compressive strength. There is addition of silica fume and metakoalin in a UHP-HFRC, not a replacement with the cement. As the size of silica fume and metakoalin is very small, it fills the pores when vibration given to the cube of 100*100mm. As the surface area increases and clogging the pores due to which the compressive strength of concrete increases.

Yu Su et al. (2017) studied the effect of silica fume, silica flour, Nano Al_2O_3 and Nano TiO_2. As the silica fume is used as a reactive material i.e. involving in the hydration process of cement. Silica flour was used to fill the pores between the aggregate and cement paste. Silica flour and other nanao materials are more finer than silica fume, due to which the pores of the material were filled with them and make them closely packed structure. And this way the compressive strength of concrete will increase.

Kou et al. (2011) observed the effect of GGBS, fly ash, metakoalin and silica fume on the mechanical properties of concrete. As the replacement of cement with silica fume and

metakoalin is done, there is enhancement in the strength from 0 to 28 days and after that there is marginal increase in the strength from 28 to 90 days.

But in case of replacement of cement with the GGBS and fly ash, there is increase in strength at a very high rate than the silica fume and metakoalin. The compressive strength of concrete decreases as there is replacement of 55% and 35% of GGBS and fly ash with the cement. Also noticed that there is increase in strength from 4 to 90 days than decreases in strength takes place. It can be concluded that fly ash and GGBS show their effect after a longer period.

Mazloom at al. (2004) studied the effect of silica fume in the concrete. There is replacement of silica fume in concrete is 0%, 6%, 10% and 15%. The increase in the compressive strength is 21% at 15% replacement of silica fume. But also noticed that in control specimen achieved the strength at 400 days is same as that of addition of silica fume in it. It can be concluded that silica fume can increase the strength for a short period of time.

a) Effect of Hybrid Fiber System

Raju et al. (2019) studied about how to develop the UHPC by using the fibers in the concrete. The variation of fibers in the concrete done to achieve the compressive strength of concrete. The total percentage of fiber used in the model is 2% in which 1% of fiber is short crimped fiber and 1.5% of fiber is long hooked fiber. As increasing the percentage 0 to 1.5% the strength increases but later on the strength decreases. Mainly long hooked fiber plays a role in the compressive strength whereas short crimped fiber resist the growth of cracks.

Yu Su et al. (2017) studied the effect of waved steel fiber, short straight fibers and twisted fibers. The aspect ratio of twisted fiber, waved steel fiber, short steel fiber 6mm length and 12mm length are 87.5, 60, 50 and 100. The quantity of steel fibers was varied from 1-2.5%. The twisted fiber will hold the concrete, waved fiber will resist the growth of cracks and the straight fiber play a role in compressive strength. With the use of these fibers the compressive strength achieved is 141 MPa.

Yu et al. (2015) studied the development of UHPC by using the binder material and fibers in the mix design according to Modified Andreasen and Andreasen particle packing model and hybridization of design of fibers. The binder content present in his model is 620 kg/m^3 which is very much lower than design model of others. The compressive strength of UHPC was achieved by adding the hybrid fibers in the concrete. The hybrid contains the short straight fibers are 0.5% of volume of concrete and long straight fibers are 1.5% of long straight fibers

and results in range of compressive strength. The figure 2.1 shows the compressive strength of specimens.

By hybridization model, the long hooked fiber mixed with short straight fiber result in increase in compressive strength as shown in the figure. As the larger quantity of short straight fiber (SSF) and lesser of long straight fiber (LHF) for the same volumetric amount then it will form homogenous concrete mix.

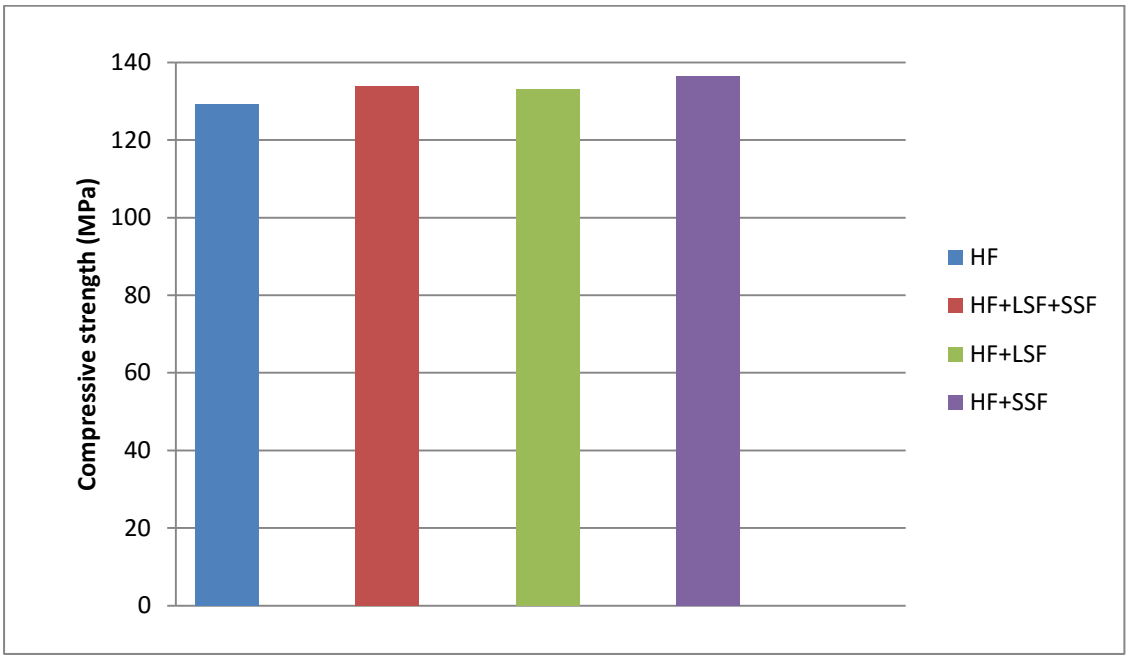

Figure 2. 8 Compressive Strength of Specimens

2.3.3 Flexural strength

The flexural strength plays an important role in the UHPFRC. The high flexural strength requires the uniform distribution of steel and dense packing. The flexural strength depend upon the orientation of the fibers. According to Steil et al. (2004), the specimen cast vertically and tested horizontally will always give less strength because of perpendicular and parallel orientation of fibers to the crack surface of horizontal and vertical specimen cast respectively.

c) Effect of Binder Material

Yu Su et al. (2017) studied the effect of silica fume, silica flour, Nano Al_2O_3 and Nano TiO_2.. The flexural strength of the specimens calculated by varying the steel fibers and nano materials as given in table 2.1.

The flexural strength depends on the nano material like aluminum oxide sample have more strength as compared to control sample i.e. there is increase in strength is 20-25%. In case of calcium carbonate, the flexural strength is increased by 20% without fiber and 0-10% increase

in strength with fibers. In case of silica oxide, the flexural strength is increased by 30% without fiber and 0-30% decrease in strength with fibers. In case of titanium oxide, the flexural strength is decreased by 85% without fiber and 0-33% decrease in strength with fibers.

Table 2. 1 Flexural Strength

Nano	Fiber					
	NO	TF1	TF2	WF	MF06	MF12
NO	10.6	14.9	x	10.8	28.1	31.3
CaCO3 3%	12.1	14.9	23.7	11	20.3	34.2
SiO2 1%	13	13	x	9.5	17	26.2
TiO2 2%	2.3	10.2	11.1	12.4	22.4	21.9
Al2O3 3%	12.4	18.7	23.5	13.2	21.4	36.1

Yardımcı et al. (2009) examined the effect of binder material on the flexural strength and also about the effect of curing scheme on flexural strength. They have used the two different curing process i.e. steam curing and autoclave curing. The strength of steam curing is lesser as compared to the autoclave curing because the steam curing results in reduction in the bond strength between the fibers and cement paste whereas the GGBS and fly ash increases the flexural strength of concrete.

Koksal et al. (2008) studied the effect of steel fiber, metakoalin and silica fume on the flexural strength of concrete. It is observed that as the silica fume increases the flexural strength also increases. As the replacement of silica fume from 0 to 15% the flexural strength increases by 65% as compared to the control specimen.

a) Effect of Hybrid Fiber System

Yu Su et al. (2017) studied the effect of waved steel fiber, short straight fibers and twisted fibers. The aspect ratio of twisted fiber, waved steel fiber, short steel fiber 6mm length and 12mm length are 87.5, 60, 50 and 100. The steel fibers are varied from 1-2.5%. The table 2.1 indicates that the steel fiber increases the flexural strength of concrete increases. The micro steel used in the material increases more strength as compare to waved and twisted fiber.

Yu et al. (2015) studied the development of UHPC by using the binder material and fibers in the mix design according to Modified Andreasen and Andreasen particle packing model and hybridization of design of fibers.

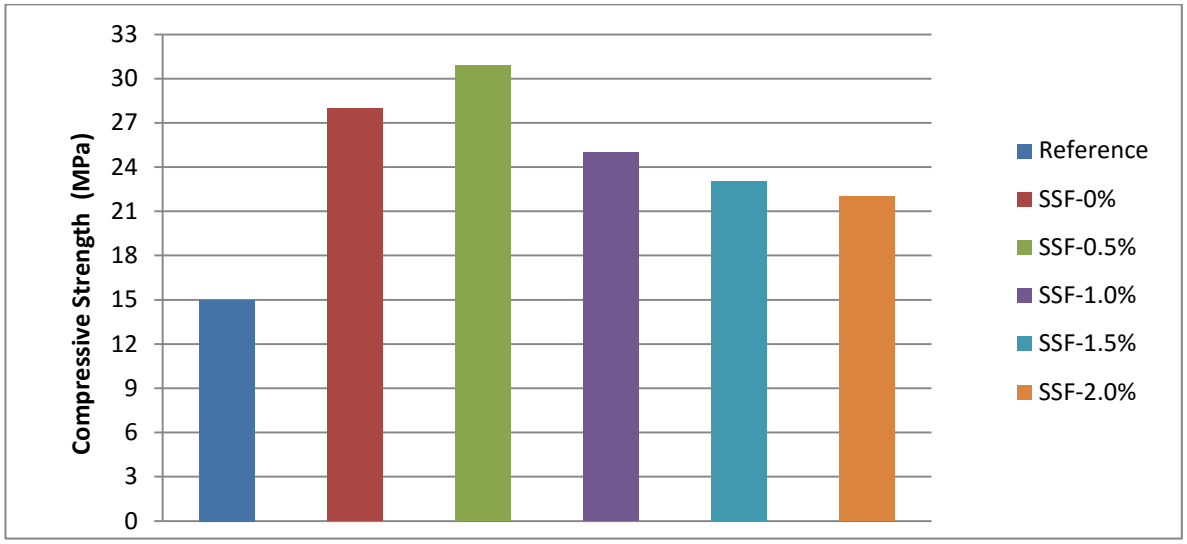

Figure 2. 9 Flexural Strength of the Mixes with Hooked and Straight Steel Fibers (Reference: UHPFRC without fibers) (Yu R. et al. 2015).

The binder content used in the concrete is 620 kg/m^3 which is very less as compared to normal mix design of UHPC. The steel fibers used in the concrete is 2% of volume of concrete i.e. short straight fibers are 0.5% of volume of concrete and hybrid long straight fibers are 1.5% of volume of concrete. The graph indicates that the value of flexural strength is maximum at 0.5% i.e. 30.9 MPa at 28 days. Therefore short straight fibers can be used with long fibers but the percentage of fiber will be 0.5%. After 0.5% short fiber, the flexural strength decreases as the value of short fiber increases in the concrete mix. The figure shows about the flexural strength of mixes with hooked and straight steel fibers.

CHAPTER 3

EXPERIMENTAL PROGRAM

3.1 MATERIAL

3.1.1 General

The compressive strength of UHP-HFRC is 100 to 150 MPa (Yu Su et al. 2018). To get the ideal compressive strength from the 100 MPa to 150 MPa (Yu Su et al. 2018), for the creation of UHP-HFRC utilizing traditionally accessible material like metakoalin, cement, silica fume, nano-silica, sand, coarse aggregates and steel fibers (hooked and crimped) were utilized. In this section, we examine about the material properties and different tests led of material for the advancement of UHPC. The examination expected to get the material properties with their outcome help to make their mix design for the strength purpose.

3.1.2 Characteristics of Material Used

As indicated by the IS code, the chemical and physical properties of different materials utilized for making UHP-HFRC decided in laboratory. The materials utilized for improvement of the UHPC are assessed to check for their acknowledgment for the creation of mix design to accomplish the strength of cement. The different materials with their considered properties which were utilized for the research are explained in the sub sections:

3.1.3 Cement

Cement is an adhesive material utilized in concrete to bind the fine and coarse aggregates. For a specific concrete mix, the determination and proper utilization of cement is significant in acquiring the ideal properties of mix. Ordinary Portland Cement (OPC) is a finely ground powder material which is produced by grinding the cement clinker. The OPC used in the research work is 43 and 53 grade. The grades describe the 28 day strength of cement. The OPC 53 cement was utilized throughout the course to make UHPC. The IS 12269:2013 code refers the specification of OPC 53 cement. As indicated by IS 12269 Common Portland cement, 53 grades will be manufactured by calcareous and argillaceous and additionally silica, alumina or iron oxide. These materials shall be burnt and grinded at a clinkering temperature. No material will be incorporated in the wake of expending, other than gypsum (normal mineral), water, execution improver(s), and not more than aggregates of total of 1.0 percent of air-entraining material, which will turn to be destructive. The cement used in the present examination was new and without any anomalies.

Figure 3. 1 OPC 53 Grade Cement

Table 3. 1 Properties of OPC 53

Characteristics	Experimental Value	Value Specified by IS 12269: 2015	Test Method Referred to
Compressive Strength (N/mm2)			IS 4031 Part 6
3 Days	34	27	
7 Days	44	37	
28 Days	62	53	
Specific Gravity	3.12		IS 4031 Part 11
Fineness (m^2/kg)	311	225	
Standard Consistency (%)	30		IS 4031 Part 4
Setting Time (min.)			IS 4031 Part 5
Initial Time (min)	135	30	
Final time (min)	195	600	
Soundness			
Le-chatlier Expansion(mm)	1	10(max)	

3.1.3 Aggregates

An aggregate occupy fifty percent of the volume of concrete and provides the dimensional stability to concrete. It provides the strength as well as also reduces the cost of concrete because it is in large amount in concrete. To make UHPC and M20 we have used two types of aggregates as classified below:

1. Fine aggregates (i.e. sand) having particle size less than 600um.

2. Coarse aggregates having size 10mm and 20mm.

Coarse aggregates help in making strong and hard mass of concrete, while fine aggregates decreases shrinkage and increase the crushing strength of concrete.

a) Fine Aggregates: Fine Aggregates are those whose particle size lies between 4.75mm to 2um. Fine aggregates depend upon area i.e. from north or from south region. The natural sand used in the research was river sand and it is from the Pathankot, Punjab and conformed that it belongs to grade-II as per IS 383 (1970). The standard sand obtained from Tamil Nadu and conformed to Grade-I as per IS 650 (1991).The standard will increase the strength in the mortar but not as useful in the concrete. Fine aggregates are used because it will help to fill the pores of aggregates and also to increase the strength of concrete. Classification of fine aggregates are:

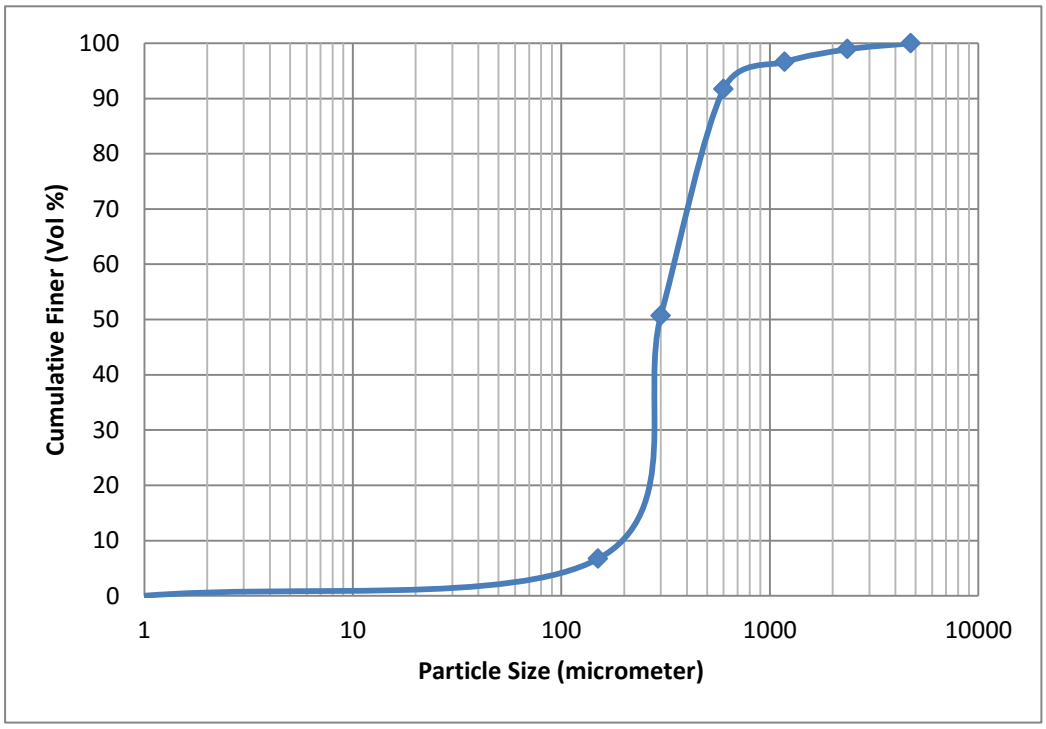

Figure 3. 2 Graph of Particle Size Distribution of Fine Aggregates

Table 3. 2 Classification of Fine Aggregates

Fine aggregate	**Size variation**
Coarse Sand	2.0mm – 0.5mm
Medium sand	0.5mm – 0.25mm
Fine sand	0.25mm – 0.06mm
Silt	0.06mm – 0.002mm
Clay	<0.002

In this research, used the medium sand and fine sand i.e. mixture of grade 1 and grade 2 sand. The sieve analysis of fine sand done in the laboratory as given below:-

Table 3. 3 Sieve Analysis of Fine Sand

Sieve size	Retained	%Retained	%Passing	Cumulative
4.75	0	0	100	0
2.36	11	1.1	98.9	1.1
1.18	23	2.3	96.6	3.4
0.6	49	4.9	91.7	8.3
0.3	410	41	50.7	49.3
0.15	440	44	6.7	93.3
0	57	5.7	1	99
Total	990	99		254.4

Fineness Modulus = 254.4/100 = 2.54

b) Coarse Aggregates: Coarse aggregates having average width 25mm and the particle size greater than 4.75mm. The aggregate whose size lies between 4.75mm to 80mm are called as coarse aggregates. These aggregates are shaped either by artificial crushing or by natural breaking down of rocks. As per the codal provisions in IS: 383-1970, states about the quality of aggregates i.e. it should be hard, durable, dense, strong, clear, free from veins and free from injurious amounts of alkali, disintegrated

pieces, vegetable matter. Flaky and elongated particles should be avoided. To make the aggregates under SSD condition and also remove the dust from the particles, the particles are firstly washed with water than dip the particles in water for 24 hours before making the concrete mix and then make the surface dry with jute bag before the use. So that it cannot absorb water during the production of concrete. The various properties of coarse aggregates are classified as

Table 3. 4 Physical Properties of Coarse Aggregates

Characteristics	**Value**
Specific Gravity	2.7
Colour	Grey
Shape	Angular
Maximum Size	10mm and 20mm

In the research work, two type of aggregates are used i.e. 20mm and10mm. The strength achieved by the 10mm coarse aggregate. The Sieve analysis of coarse aggregates (10mm) done in the laboratory as given below:-

Table 3. 5 Sieve Analysis of Coarse Aggregates

Sieve	Mass	% Retained	% Passing	Cumulative
80	0	0	100	0
40	0	0	100	0
20	0	0	100	0
10	2.44	48.8	51.2	48.8
4.75	2.14	42.8	8.4	91.6
0	0.42	8.4	0	100
			Total	240.4

Fineness Modulus = (240.4+500)/100 =7.4

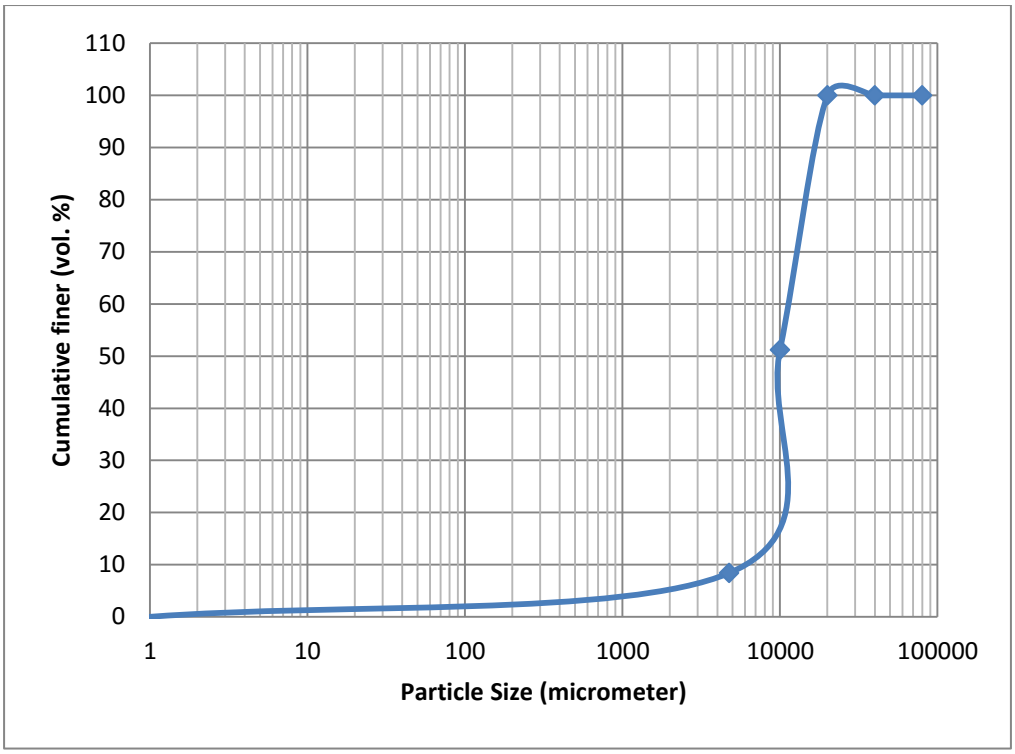

Figure 3. 3 Graph of Particle Size Distribution of Coarse Aggregates

3.1.4 Metakoalin

Metakoalin was utilized in the design mix as additional material against cement to study its effectiveness for the improvement of UHP-HFRC. It is obtained from "KAOMIN Industries". The table shows the physical properties of metakoalin.

Table 3. 6 Physical Properties of Metakoalin

Amorphous Content	>90%
Dosages	5 to 22% of Cement weight
Average Particle size	0.8µ - 1.2 µ
Bulk Density (gm/ltr)	320 to 350
Specific Gravity	2.6

It is in white colour, unique pozzolana with highly reactive. It is processed from kaolinite rich clay and observed under the precise calcination temperature to get best pozzolanic additive. It is specially used for high end concrete and aesthetic concrete application. It helps to enhance the workability of the concrete. While adding the metakoalin in cement will reduce the water cement ratio and also increase the strength of concrete. The table shows the chemical properties of metakoalin.

Table 3. 7 Chemical Properties of Metakoalin

SiO_2 + Al O	Fe2O3	Alkaline Impurities	Loss On Ignition
>95.0%	<0.5%	<0.8%	<1.5%

3.1.5 Silica Fume

Silica Fume is a highly reactive pozzolanic material which is used as replacement of cement. It is also known as Condensed Silica fume. It increases the durability of concrete and increases its strength. The individual particles are very small and approximately 1/100th the size of an average particle of cement. Due to its fineness of silica fume, it fills the voids between coarse aggregates, cement and fine aggregates making the mix more impermeable and dense. The silica fume utilized in this project was obtained from KGR Agro Fusions (P) Ltd., Ludhiana Punjab. These are the codes ASTM C 1240 and AASHTO M 307 specify the quality of silica fume. The properties of silica fume were provided by KGR Agro Fusions (P) Ltd are:-

Table 3. 8 Physical Properties of Silica Fume

Particle size (typical)	< 1 μm
Specific Gravity	2.4
Color	Bluish Grey
Bulk Density	550-700 kg/m3
Specific Surface	15,000 to 30,000 m2/kg

Table 3. 9 Chemical Composition of Silica Fume

SiO_2	MgO	SO_3	H_2O	K_2O	Na_2O	CaO	Si	Cl	Fe_2O_3
92.25%	<1.5%	<1.1%	<0.4%	<2.25%	<1.4%	<0.35%	<0.5%	<0.06%	<2%

3.1.5 Nano Silica

Nano silica is in liquid form and it affects the properties of concrete mix because of high purity (greater than 99%) and high specific area. The particle size of nano silica is much smaller than silica fume and metakoalin particles. The nano silica used in our study was manufactured by BEECHEMS, Kanpur. Nano silica used in the research is a white translucent liquid (like a water) having no odour. The table 3.10 shows the physical properties of nano silica.

Table 3. 10 Properties of Nano Silica

Specific Gravity	1.2-1.6
Particle size	1-100nm

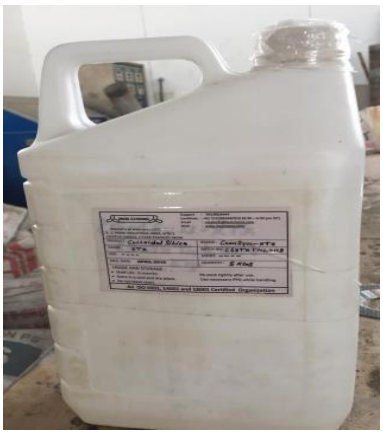

Figure 3. 4 Nano Silica

3.1.6 Steel Fibers

To make UHPC concrete we use two types of steel fibers:-

a) Crimped Fiber
b) Hooked Fiber

These steel fibers provide the strength to concrete. Mostly it will increase the strength near about 20 to 25% strength. But it will decrease the workability of concrete. Crimped fiber will help to delay the propagation of cracking in the concrete. Hooked fiber will take more load as it will increase the strength of concrete. The steel fibers used in the research obtained from the "KASTURI STEEL FIBERS, NAGPUR" AND "SHAKTIMAAN STEEL FIBERS". The steel fibers used in the research work , i.e. 2.5% of the volume of concrete in which 1% are crimped steel fiber and 1.5% are hooked steel fiber. The properties of steel fibers are:-

Table 3. 11 Properties of Steel Fibers

Company Name	**Type of fiber**	**Aspect ratio**	**Length (mm)**	**Diameter (mm)**	**Ultimate tensile strength (MPa)**
Kasturi Steel Fibers	Crimped fiber	25	15	0.6	1200
	Hooked fiber	80	60	0.75	1200
Shaktimaan Steel Fibers	Crimped fiber	45	13	0.3	900
	Hooked fiber	85	50	0.6	900

a) Short Crimped Fiber (SCF)

b) Long Hooked Fiber (LHF)

c) Length measurement of SCF of ‘KSF’

d) Length Measurement of LHF of ‘KSF’

e) Length measurement of SCF of ‘SSF’

f) Length Measurement of LHF of ‘SSF’

Figure 3. 5 Different fibers used in UHP-HFRC

3.1.7 Super-Plasticizer

Normet Tanchem H3 is used as a super plasticizer to make UHPC. It is a poly-carboxylic ether based and free from chloride and alkali. It is used to increase the durability of the concrete which will primarily help to develop the ultra-high performance concrete. This super plasticizer is compatible with all other concrete.

3.1.8 Carbon Fiber Reinforced Polymer

CFRP is a light weight fiber and it is extremely strong. It is used where high strength to weight ratio and stiffness required. The binding material required for the CFRP to make mesh type structure with epoxy i.e. “Sika – Sikadur 330 (in) Comp.A”. The size of the mesh used in the 25mm*25mm.

Figure 3. 6 CFRP Sheet

Table 3. 12 Properties of CFRP

Sr. No.	Physical Properties	Value
1.	Modulus of Elasticity (GPa)	240.0
2.	Tensile Strength (MPa)	3800
3.	Density (gm/cm^3)	1.7
4.	Thickness (mm)	0.12
5.	Weight of CFRP mesh, after stitching (gsm)	230.0
6.	Weight of CFRP mesh before stitching (gsm)	200.0

3.1.9 Sikadur 330 Epoxy

The epoxy used in this project is obtained from the “Sika Pvt. Ltd.” The epoxy contains resin i.e. of white colour and hardener i.e. of black colour. The density of epoxy is 1.3 kg/l + 0.1 kg/l (at +30°C). It has high mechanical properties.

Figure 3. 7 Sikadur epoxy i.e. Hardener and Resin

3.1.10 Stress-Strain of M20

The graph shows the stress strain curve of control sample at 28 days i.e. M20 mix design done on the CTM machine. It indicates that with an increase in stress on the cylinder i.e. 150*300mm then how strain variation will takes place.

Figure 3. 8 Testing of Cylinder on CTM to calculate stress strain graph

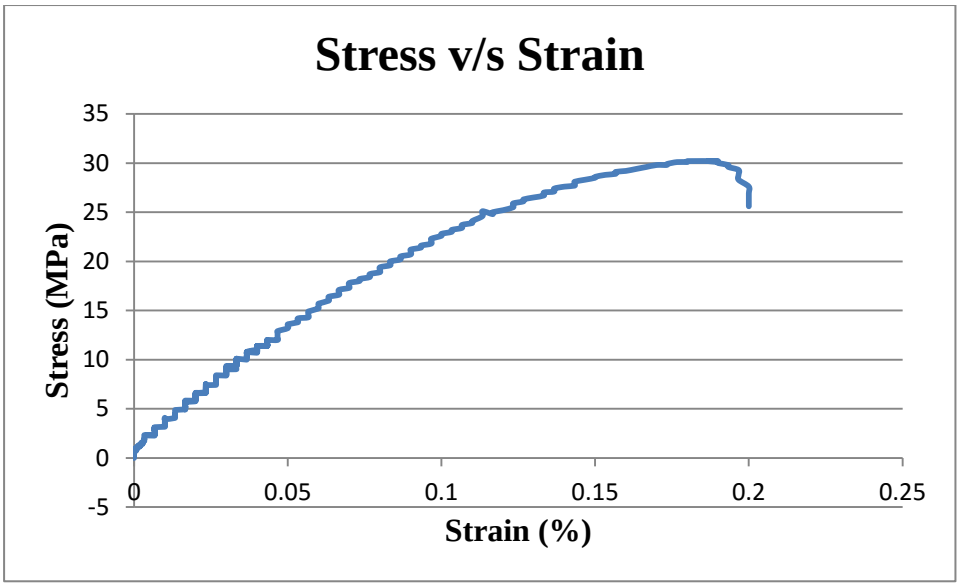

Figure 3. 9 Stress Strain Graph of M20

3.1.11 Tensile Strength

In this section, check the tensile strength of the reinforcement. Tensile strength of reinforcement can be checked on the Universal Testing Machine. It tells about the capacity of the material or at which load it tends to elongate the bar. Also indicates about the cracking pattern of reinforcement and stress strain curve. The highest point on the curve shows the ultimate tensile strength of reinforcement. It is measured in the form of force per unit area. The stress strain of 8mm and 10mm reinforcement graph are shown in figure 3.11 and 3.12.

a) Breaking of Reinforcement b) Fracture of Reinforcement at 45^0

Figure 3. 10 Testing of steel reinforcement

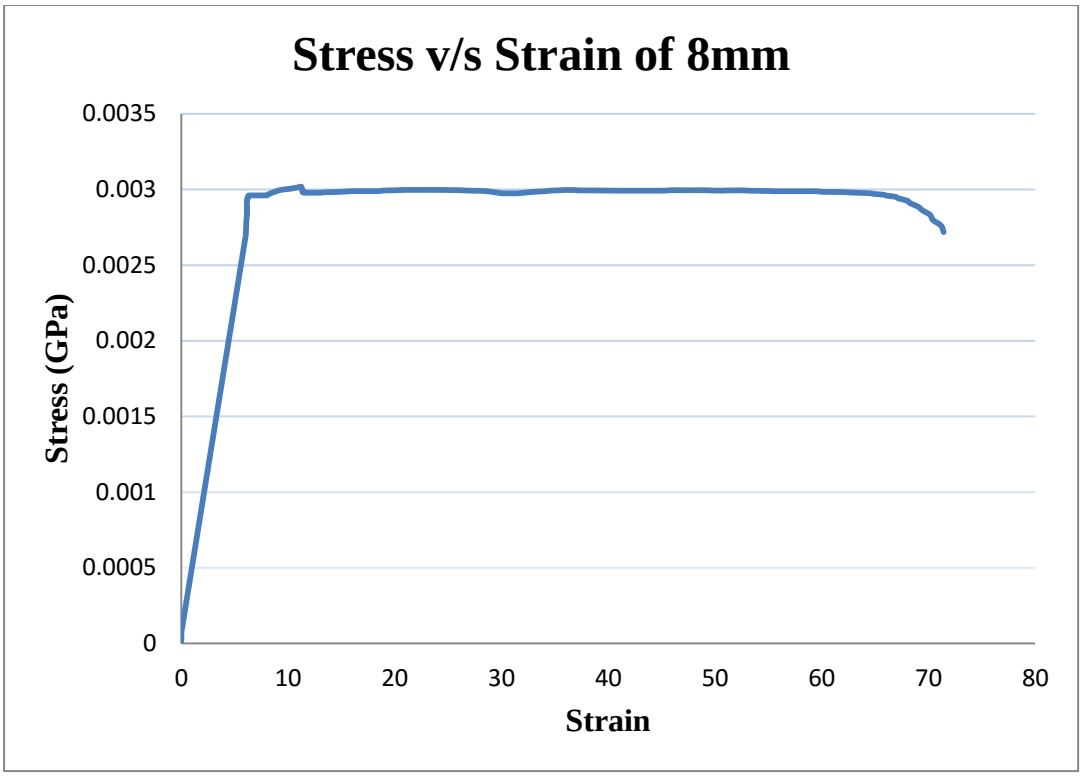

Figure 3. 11 Stress Strain Graph of 8mm steel

The figure 3.11 shows that the 8mm reinforcement achieved the 0.003 GPa stress and reached the ultimate strain of 71.17. In figure 3.12, the 10mm reinforcement achieved the 0.0056 GPa stress and reached the ultimate strain of 64.87.

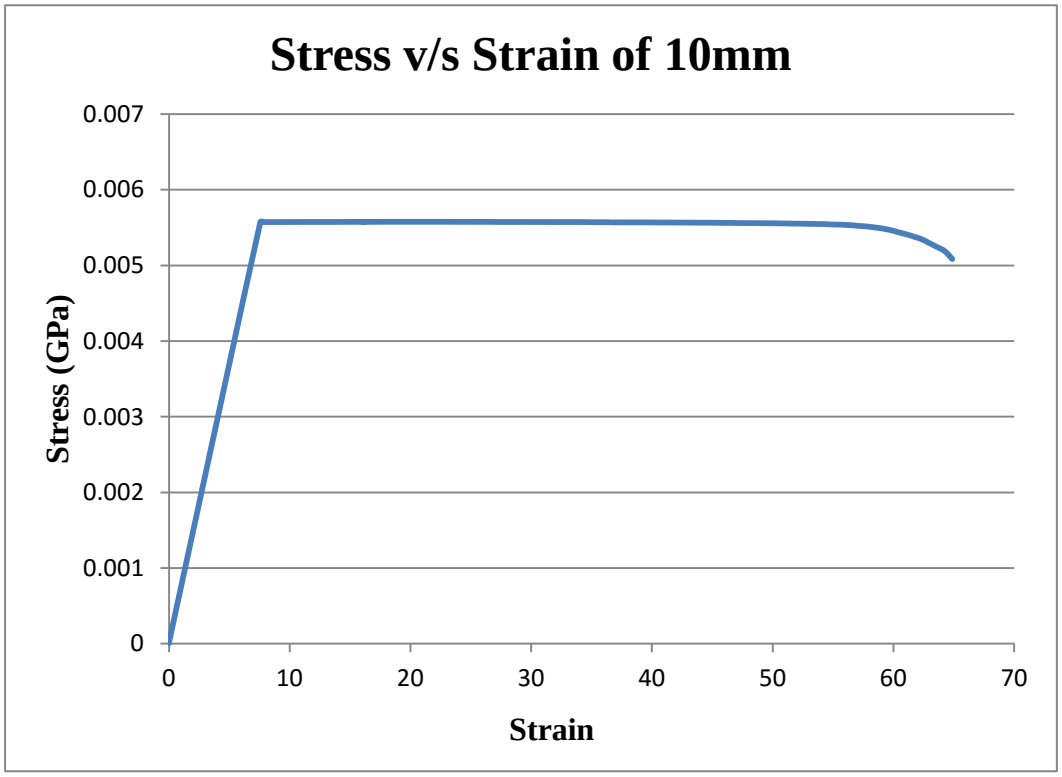

Figure 3. 12 Stress Strain Graph Of 10mm

3.2 DEVELOPMENT OF ULTRA-HIGH PERFORMANCE HYBRID FIBER REINFORCED CONCRETE

3.2.1 Preparation of Sample

The constituent materials for UHP-HFRC were weighted as per mix design. The material used in UHPC is OPC 53 cement, silica fume, metakoalin, super plasticizer, hooked fiber, crimped fiber, nano silica, sand, coarse aggregates, water.

Firstly, we will mix the powder material like cement, silica fume, metakoalin for 5 minutes. Then mix the sand and coarse aggregates with powder mix for 5 minutes. Then add the some hooked and crimped fiber in material and mix for some time. Then put the material in the small concrete mixture, add the 30% of the volume of water in the mixture and rotate the mixture for 1 minute. After 5 cycles of rotation completed, then add some super plasticizer and Nano silica in the mixture and again add water after 5 cycles completed. Also sprinkle the hooked and crimped steel fiber in the mixture when mixer is rotating.

After proper mixing, pour the mix in the oiled moulds of cube size of 100mm*100mm for compression test. Then give some vibration to the cubes for uniformly distribution and it doesn't require any surface finishing. At the end cubes are covered with jute bags for 24 hours. After 48 hours open the moulds and put into the curing tank whose temperature of water tank is 23 ± 2^{o} C. The specimens kept in the water tank until the test day will come. The key factors for UHP-HFRC are:

1. Cement content 950kg/m^3, silica fume content (15% of cement) and metakoalin content (10% of cement) is used as binder material.
2. The total content of steel fibers is 2% where 1% is short crimped fiber and 1.5% is long hooked fiber.
3. Coarse aggregates cement ratio will be 1 because by increasing the value of coarse aggregates the paste value decreases in the material.
4. Water binder ratio will be decreased from 0.25 to 0.2 expectedly it will increase the compressive strength of concrete.
5. Super plasticizer binder ratio also decreased from 2.5% to 2% because the concrete cube moulds take more time than 48 hours.

3.2.1 Mix Design of UHP-HFRC

In this chapter, we will discuss about the procedure of UHP-HFRC. There are many trials done to prepare UHP-HFRC by varying quantity of materials. The compressive strength of concrete checked at 7 days and 28 days by changing the proportions of material.

The quantity of Silica fume is used in mix design is 15% of the weight of the cement and metakoalin is 10% of the weight of cement. The content of super plasticizer variation between the 2 – 2.5% of weight of binder material and the content of water is 0.19 to 0.25 of weight of binder material.

Steel fibers used in the research have different sizes i.e. there aspect ratio, diameter, length, strength are varying. The aspect ratio of crimped and hooked fiber of shaktimaan fiber is 45 and 85. The aspect ratio of crimped and hooked fiber of kasturi fiber is 25 and 80. In research work, used two different sand those who are passing from 600um and normal sand i.e. un-sieved sand. The size of coarse aggregates used in the mix design is 10mm. Coarse aggregates and cement ratio varying between 0.8 to 1.35.

3.2.2 Advantages of UHP-HFRC

1. Mechanical properties like compressive strength, flexural and tensile strength are excellent.
2. Very low permeability and acts like hard or aggressive solution.
3. Provides a good bonding and perform better than older material.
4. Durability properties of UHP-HFRC are outstanding.
5. It requires less material as compared to normal reinforced concrete.
6. It is a self-compacting concrete.

3.2.3 Problems Faced for the Development of UHP-HFRC

a) In the starting of making UHPC, the main problem faced that it is not easy to achieve the workability of concrete because water binder ratio is very less i.e. 0.2. Due to this the balls were formed in the mixer. The mixing of mortar properly done in the Hobart mixer because the speed of mixer is controllable, fast and entrainment of air reduce the effect of super-plasticizer also.

b) At the time of mixing, long hooked fibers will form bundling of fibers and the size of the mould is 100mm*100mm and the size of long hooked fibers is 60mm. These fibers make a bundles at the time of placing of concrete in the mould, due to the fibers. The

portion where it will rest or form bundle, the portion will become weak. That's why compressive strength of concrete will decrease.

c) It will take 48 hours to open the mould and on the other side other concrete mixture will take 24 hours to open the mould.

d) In the design C7, cement content is increased from 950 to 980kg/m^3, it takes 72 hours to harden the surface plus the outer surface of the concrete falls down because the demoulding the mould before 72 hours.

e) In compression test, one of the major observation is failure pattern and disadvantages of Ultra high performance is that it is brittle in nature. When load applies on the cube, it will fail immediately or there is sudden explosion takes place when it reaches to peak load.

Figure 3. 13.Balling effect during mixing of mortar in the mixer and Bundling of fibers

Figure 3. 14 Condition of Mix 7 of concrete i.e cement content 980kg/m^3

Table 3. 13 Trial Mix of Mortar

S.No.	CEMENT (kg/m^3)	SAND (600um) (kg/m^3)	SF (kg/m^3)	METAKOLIN (kg/m^3)	NS %	FIBER		W/B RATIO	SP/B	Compressive strength (MPa)		ASPECT RATIO	
						Cr.	H			7DAYS	28DAYS	CRIMPED	HOOKED
M 1	950	1050	143	95		78	117	0.25	2.5	60	72	45	85
M 2	950	1050	143	95		78	117	0.23	2.5	65	76	45	85
M 3	950	1050	143	95		78	117	0.2	2.5	76	92	45	85
M 4	950	1030	143	95		78	117	0.2	2	80	93.65	45	85
M 5	950	1030	143	95	2	78	117	0.2	2	82	96	45	85
M 6	**950**	**1030**	**143**	**95**	**2**	**78**	**117**	**0.2.**	**2**	**87**	**109**	**25**	**80**

Table 3. 14 Trial Mix of Concrete

S.No.	C (kg/m^3)	SAND (600um) (kg/m^3)	N.S. (kg/m^3)	C.A. 10mm / CEMENT	SF (kg/m^3)	M (kg/m^3)	NS %	FIBER		W/B RATIO	SP/B	Compressive strength(MPa)		A.S.	
								Cr.	H			7 DAYS	28 DAYS	Cr.	H.
C 1	950		1050	0.8	143	95		78	117	0.2	2.5	70	88	45	85
C 2	950		1050	1	143	95		78	117	0.2	2	85	106	45	85
C 3	950		1050	1.1	143	95		78	117	0.2	2	84	101	45	85
C 4	950	1050		1.2	143	95		78		0.2	2	80	94	45	85
C 5	950		1050	1.35	143	95		78	117	0.2	2	X	X	45	85
C 6	**950**	**1030**		**1**	**143**	**95**	**2**	**78**	**117**	**.2.**	**2**	**97**	**122**	**25**	**80**
C 7	980	1030		1	143	95	2	78	117	.2	2	95	112	25	80

*N.S. Normal Sand, NS Nano Silica, C.A. Coarse Aggregate

As the table depicts that the compressive strength of mortar or concrete depends mainly on hybrid fiber aspect ratio. In the starting the aspect ratio of crimped fiber is 45 and 85 due to more aspect ratio it couldn't achieve his strength. After that some changes in aspect ratio taken due to which there is increase in strength i.e 10-15% more as compared intial steel fiber.

From the tables 3.13 and 3.14, the mortar mix 6 and concrete mix 6 shows the better performance. The value of compressive strength of concrete is more as compared to the mortar. The workability of concrete is much better than the workability of mortar. So that's why concrete mix design used for the retrofitting process.

In figure 3.15 - 3.16, depicts the mean of 28- compressive strength of UHP-HFRC samples of one mix and also shows the error between their values.

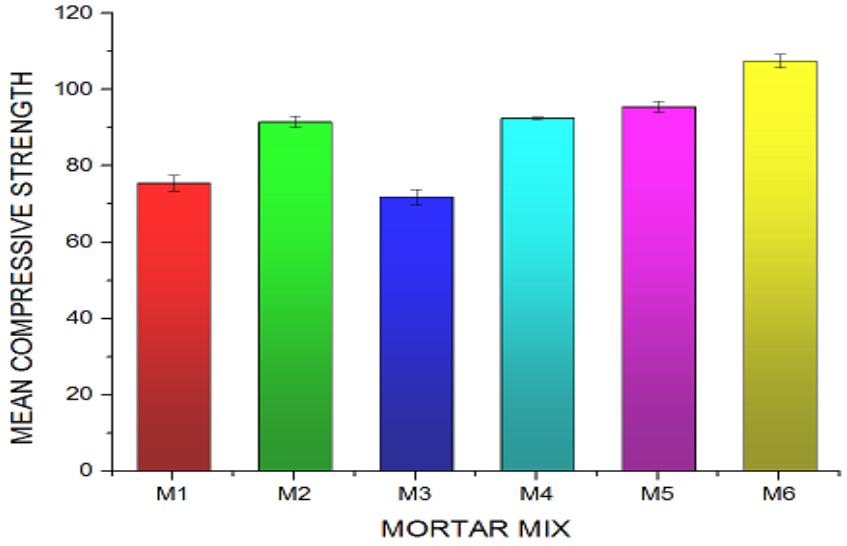

Figure 3. 15 Mean compressive strength and S.E. of mean of mortar mix

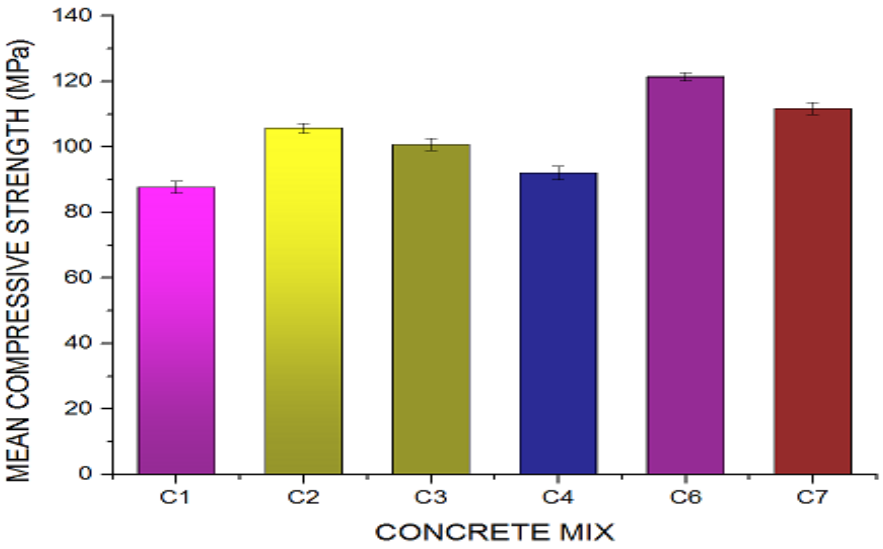

Figure 3. 16 Mean compressive strength and S.E. of mean of concrete mix

Table 3. 15 Mean Compressive Strength and S.E. of Mean

MIX	MEAN C.S (MPa).	S.E. OF MEAN	MIX	MEAN C.S. (MPa)	S.E. OF MEAN
M1	75.67	2.03	**C1**	87.67	1.85
M2	91.67	1.45	**C2**	105.67	1.45
M3	72	2.08	**C3**	100.67	1.85
M4	93.67	0.33	**C4**	92	2.08
M5	95.67	1.45	**C6**	121.33	1.20
M6	108.67	1.85	**C7**	111.67	1.85

*C.S. Compressive Strength, S.E. Standard Error

Table 3. 16 Mix Design of Mortar and Concrete

Materials	UHP-HFRC (Mortar) (kg/m^3)	UHP-HFRC (Concrete) (kg/m^3)
Cement	950	950
Silica fume	143	143
Metakoalin	95	95
Sand	1030	1030
Aggregates		950
Water/ binder ratio	0.2	0.2
Super plasticizer/ binder ratio	0.02	0.02
Crimped steel fibers	78	78
Hooked steel fibers	117	117

According to table 3.16, there are two mix design for the UHP-HFRC i.e. mortar and concrete. The concrete mix design is used for the retrofitting of BCJ. The proportions of the UHP-HFRC shown in the table 3.17.

Table 3. 17 Mix Proportion of UHP-HFRC

Ingredient	Cement	S.F.	Metakoalin	Sand	C.A.	w/b	SP/B	Steel fibers	
								Cr.	H.
Proportion	1	0.15	0.1	1.084	1	0.2	0.02	0.0821	0.123

3.3 PREPARATION OF BEAM COLUMN JOINT

3.3.1 Casting of Beam Column Joint

For the development of the beam column joint firstly decide the size of the beam and column. Then decide which type of concrete poured in the BCJ i.e. M20. Then design the beam column joint reinforcement according to the load.

The cross section of specimen used in the experimental program, the size of beam is 225mm*125mm with an overall length of 950mm and cross section of column is 225mm*125mm with an overall length of 1000mm. The cover blocks of 25mm used in the T beam column joint placed under the reinforcement.

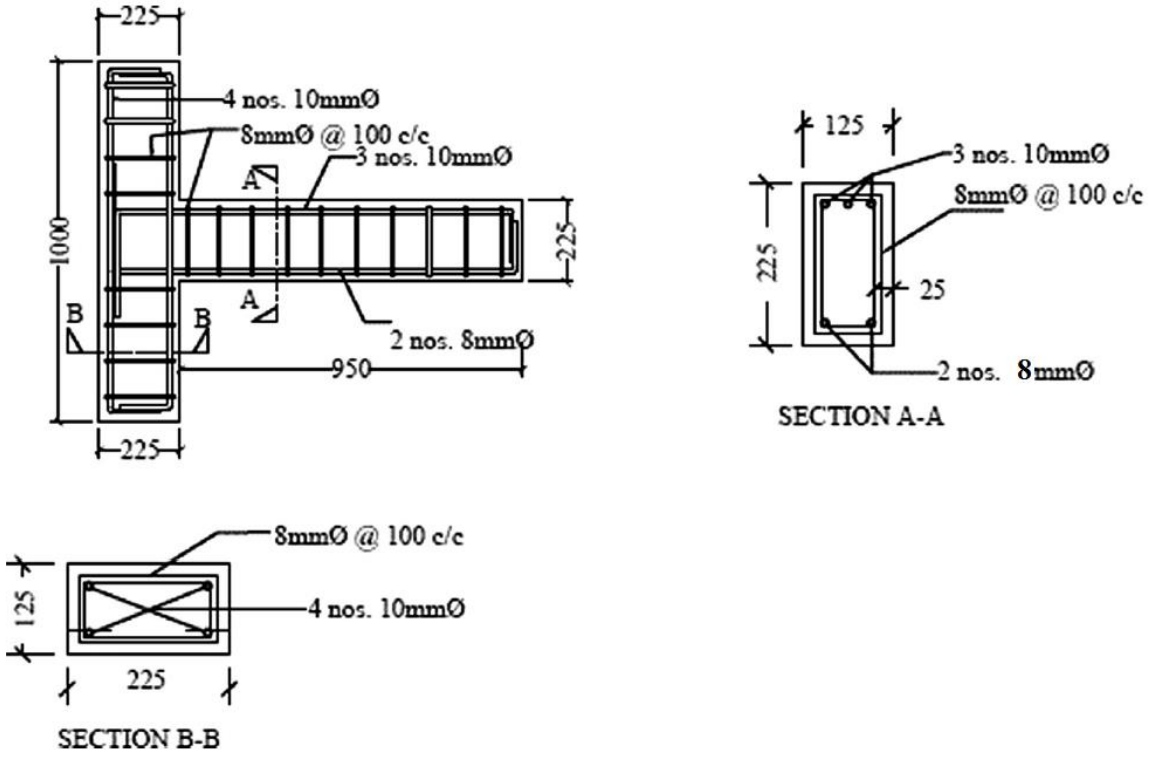

Figure 3. 17 Reinforcement detail of BCJ (sharma et al.2019)

The detailing of the reinforcement cage is that the reinforcement of column is 4 bars of 10mm dia. i.e. all the bars provided on the corners of the column and the stirrup are provided of 8mm

diameter and spacing provided between the stirrups is 100mm. The reinforcement of beam on the tension side is 2 bars 8mm and on the compression side is 3 bars of 10mm and stirrups are provided of 8mm diameter and the spacing provided between the stirrups is 100mm. Mix design of M20 as per Indian Standard code 10262:2009 in table 3.18 and the compressive strength achieved by material is 29.8MPa.

Table 3. 18 Material of M20

MATERIAL	QUANTITY
CEMENT	394kg/m^3
SAND	637kg/m^3
COARSE AGGREGATES 10MM	456.8kg/m^3
COARSE AGGREGATES 20MM	685.2kg/m^3
WATER	197kg/m^3

After designing the reinforcement, then prepare the mix M20 according to IS 10269:2009. Then mix the cement, sand, coarse aggregates and water as per proportions obtained from the design mix. Firstly do the oiling of the T beam column joint mould with brush then placed the reinforcement in the mould and also place the cover blocks under the reinforcement. Then pour the concrete over the reinforcement and simultaneously use the needle vibrator for compaction purpose. The compaction done till the t beam is filled completely. After that place it for 24 hours so that concrete will be set in mould. Then de-mould the mould and place it for the curing process for 28 days..

a) Reinforcement Cage in Moulds

b) Compaction of Concrete using Vibrating Needle

c) Beam Column Joint

Figure 3. 18 Preparation of control specimen

3.3.2 Testing Arrangement

All the control specimen and retrofitted specimen tested under servo control hydraulic jack. The load cannot be controlled on the actuator machine that's why controlling the displacement. The load is applied in the cyclic form, in which hydraulic jack moves +5mm and come back to its initial position then -5mm. repeat the each cycle for two times and continue the process according to their damage index level.

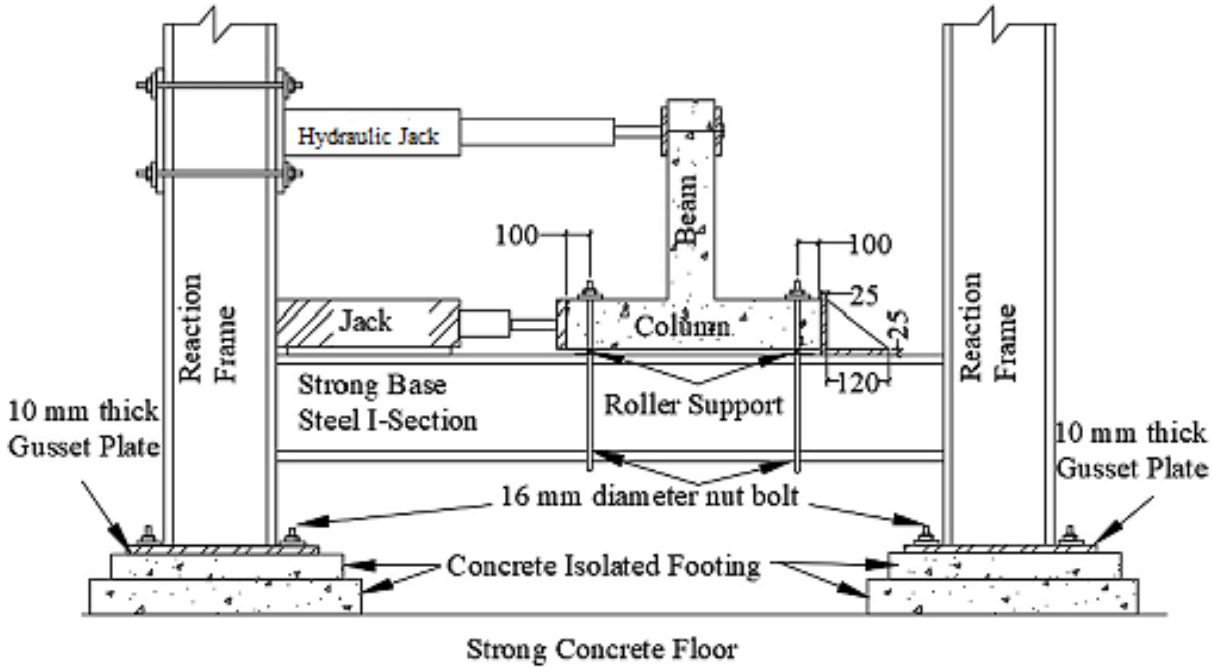

Figure 3. 19 Testing Arrangement of T Beam Column Joint (Raju et al. (2019)

Place the column horizontally and beam vertically. The plates are fixed at 100mm from both end side of column with the 16mm diameter nut bolt so that it will not overturn and displace from its position.

Firstly calculate the axial load on the column according to code SP-34 i.e. area of reinforcement in the BCJ is known. Calculate the load from the IS code Sp-34 with respect to area of reinforcement. In IS code sp-34, the clause says that axial load on the column is 10% of the load carrying capacity of column.

Then fit the hydraulic jack on the beam at a distance of 100mm from the top of beam. The deflection at a point of 100mm from the top of beam corresponding to load can be calculated with the help of LVDT (linear variable displacement transducer). Two LVDT's were used on both side of the beam and the initial value on the LVDT's is 0 mm and maximum value is 50mm. The two roller supports are placed below the column and check whether the LVDT initially at zero or not.

3.3.3 Methodology

In this chapter, studied about at what damage level beam column joint will be cracked and how to retrofit the T beam column joint by CFRP jacket and also about UHP-HFRC concrete.

Firstly control specimen tested under quasi-static reverse cycle loading till its ultimate displacement or failure point. Then from load displacement curve, calculate the damage index level by park and ang index model which will indicate the four damage level i.e. complete damage, severe damage, moderate damage and slightly damage. Park and Ang index model is :-

$$D = \frac{\delta_m}{\delta_u} + \frac{\beta}{\delta_u F_y} \int dE$$

In this $\delta_u$is the ultimate displacement and $\delta_m$is the maximum displacement considered. β is the strength degradation parameter whose value is 0.1. F_y is the yield strength of structure whose value is calculated from the load displacement hysteresis graph shown in figure 3.20.

F_y can be calculated from the s- curve of complete damage i.e. check the peak load from s-curve and multiply the peak value with 0.8. Each damage index can be calculated from hysteresis graph of complete damage by applying the quasi static loading.

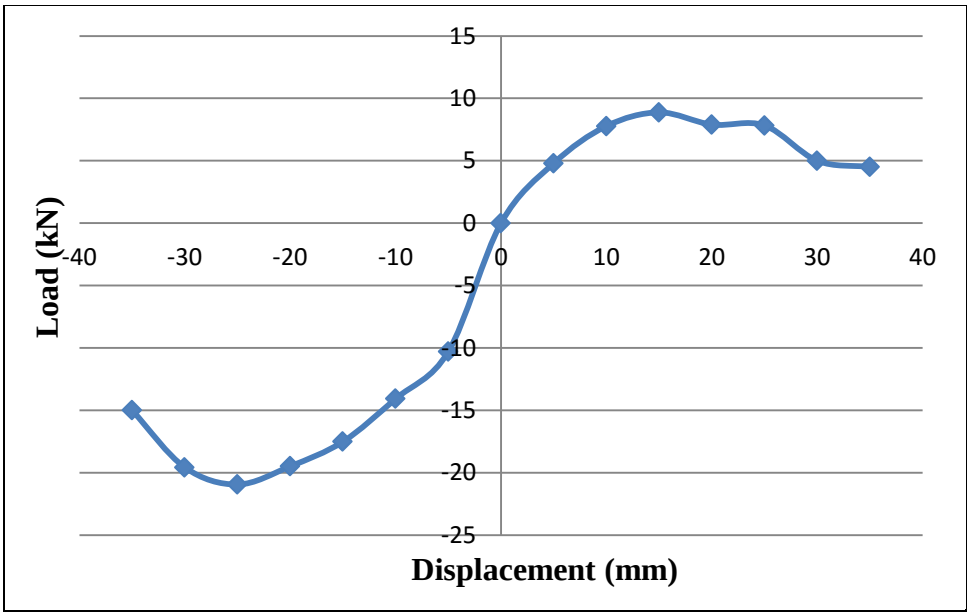

Figure 3. 20 Load Displacement Envelope of Control BCJ

From this graph, 0.8 * peak load will be 14.90817.

dE is the cumulative hysteresis energy dissipation of cycle. Therefore, calculate the energy upto 35mm and each cycle will increase by 5mm.

For 5mm $D = \frac{5}{35} + \frac{0.1*32.016}{35*14.91} = .14$

For 10mm $D = \frac{10}{35} + \frac{0.1*98.13}{35*14.91} = .308$

For 15mm $D = \frac{15}{35} + \frac{0.1*175.8}{35*14.91} = .47$

For 20mm $D = \frac{20}{35} + \frac{0.1*300.84}{35*14.91} = .629$

For 25mm $D = \frac{25}{35} + \frac{0.1*461}{35*14.91} = .80$

For 30mm $D = \frac{30}{35} + \frac{0.1*405}{35*14.91} = .93$

For 35mm $D = \frac{35}{35} + \frac{0.1*300}{35*14.91} = 1$

For damage index, theoretical range of slightly damage is 0.2-0.4, for moderate is 0.4-0.6, for severe is 0.6-0.8 and for complete damage is 1.

Therefore, the nomenclature of damage index of BCJ is:-

1. The damage index of slightly damaged BCJ is 0.308.
2. The damage index of moderate damage is .47.
3. The damage index of severe damage is 0.8.
4. The damage index of complete damage is 1.

The damage index indicates that how much specimens are required for testing. The number of specimens is prepared for the testing are eight in which all damage level have 2 specimens. After calculating the damage index of beam column joint then beams are tested under quasi static loading upto the severe damage, moderate damage and slightly damage. The chipping process has done near the joint part i.e. to remove concrete upto the reinforcement of BCJ by making an angle of 45^{o} of chisel with horizontal. Remove the concrete 625mm from the joint along the beam side and 312.5mm from center of column on both sides.

3.3.4 Retrofitting Scheme

Mostly CFRP placed at the joint in the form of laminates in published papers which will de-bond at the time of testing but it will prevent from spalling of concrete. In our research, the main aim is to reduce the use of CFRP and make them economical. So that's why providing the CFRP in the strips form which will reduce the use and make them economical. The CFRP mesh is sandwiched between the two layers of concrete. The aesthetic point of view it looks good and there is no de-bonding at BCJ of take place.

Cut the CFRP sheet into strips of 25mm width and make a mesh of 25mm * 25mm. The size of mesh of CFRP is 25mm taken because coarse aggregates used in the UHP-HFRC is 10mm and use of fibers are there. The size of mesh is small then it will hinder the path of concrete. The size of strips used in the retrofitting is 1500mm*25mm and 600mm*25mm.

a) b)

Figure 3. 21 Chipping of BCJ and Fixing of CFRP Mesh

Use the Sikadur 330 epoxy at joints of CFRP so that horizontal and vertical strips do not displace from their position. Leave it for 4 to 5 hours so that displacement of strips do not take place. Then use Nito-bond on the surface of chipped portion so that old and new concrete make a strong bond.

After that oil the BCJ with brush and place the retrofitted BCJ in the mould and tighten all the screws. Then make UHP-HFRC in small mixture and place the concrete mix on the chipped portion. Then use the table vibrator for the compaction of concrete till the BCJ is completely filled. After that put the wet jute bag on the beam column joint so that inside water in the mix will not disappear and stops the hydration process of concrete. After 48 hours demould the mould carefully and put the retrofitted BCJ for the curing process i.e by putting the wet jute bags on the surface of BCJ.

Figure 3. 22 Placing and Concreting of BCJ

3.3.5 Properties of BCJ

The various properties of BCJ are calculated by testing the BCJ under seismic loading condition. The properties of BCJ are load displacement curve, displacement ductility, peak to peak stiffness, energy dissipation, moment rotation and principle joint tensile stress.

The load displacement hysteresis curve tells about the behavior of BCJ and also about the ultimate load carrying capacity of the BCJ and how much ultimate displacement can take place. Through load displacement curve, S curve can be developed by plotting maximum value of each cycle and by calculating the ultimate displacement and yield displacement from

S curve, the ratio of ultimate displacement and yield displacement is called displacement ductility.

The load displacement curve will help to calculate the energy dissipation of BCJ in which area enclosed in the load displacement hysteresis loop at different drift ratio is called energy dissipation. The energy dissipation indicates the structural response during earthquake.

The stiffness of BCJ can be calculated from load displacement curves i.e. ratio of load and displacement. As the damage level increases the stiffness of the specimen decreases. In result and discussion chapter, the graph plotted between the peak to peak stiffness of the specimen and drift ratio. Drift ratio is defined as the ratio of maximum drift divided by total height of specimen.

The moment can be calculated from product of load and height of specimen. The rotation is calculated from maximum drift divided by total height of specimen. The principle joint tensile stresses are calculated by using priestly equations. All these properties are calculated for control specimen as well as for the retrofitted specimen.

CHAPTER 4

RESULTS AND DISCUSSION

4.1 General

This chapter deals with the results obtained from the various properties from the mechanical test performed on Ultra High performance hybrid steel concrete. In this chapter, trials are done for making the UHPC are based on the compressive strength and the workability of the concrete and mortar.

4.2 Compressive Strength

The compressive strength of the cube can be calculated with the help of CTM. The average value of compressive strength of 3 cubes of UHPC at 7 days and 28 days showed in the table 3.13 and 3.14. The compressive strength of 7 days is 65-75 % of 28 days. The strength of the concrete depends on the hydration of cement. As the hydration of cement is more than the strength of concrete will also more. The compressive strength of mortar increases from 72 MPa to 109 MPa. In case of concrete, there is variation in the coarse aggregate cement ratio i.e. it changes from 0.8 to 1.35 and achieved the strength at ratio is 1:1. The compressive strength of concrete increases from 88 MPa to 122 MPa as shown in figure 4.2.

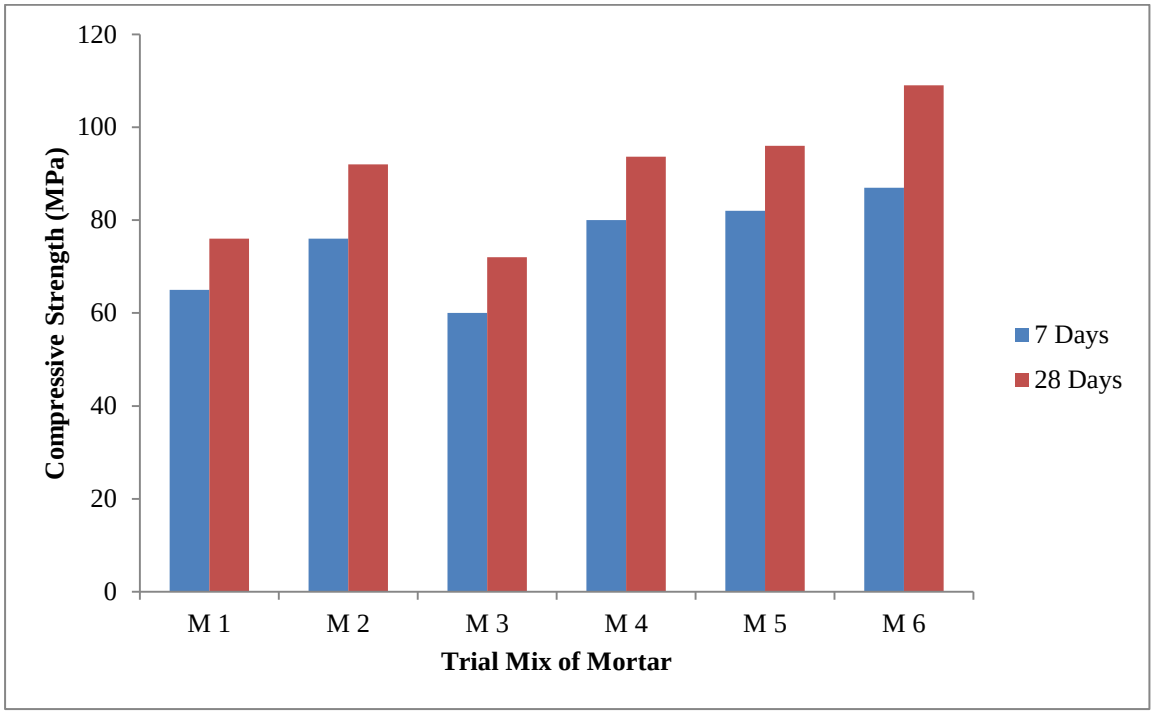

Figure 4. 1 Compressive Strength of 7 days and 28 days of UHP-HFRC Mortar Mix

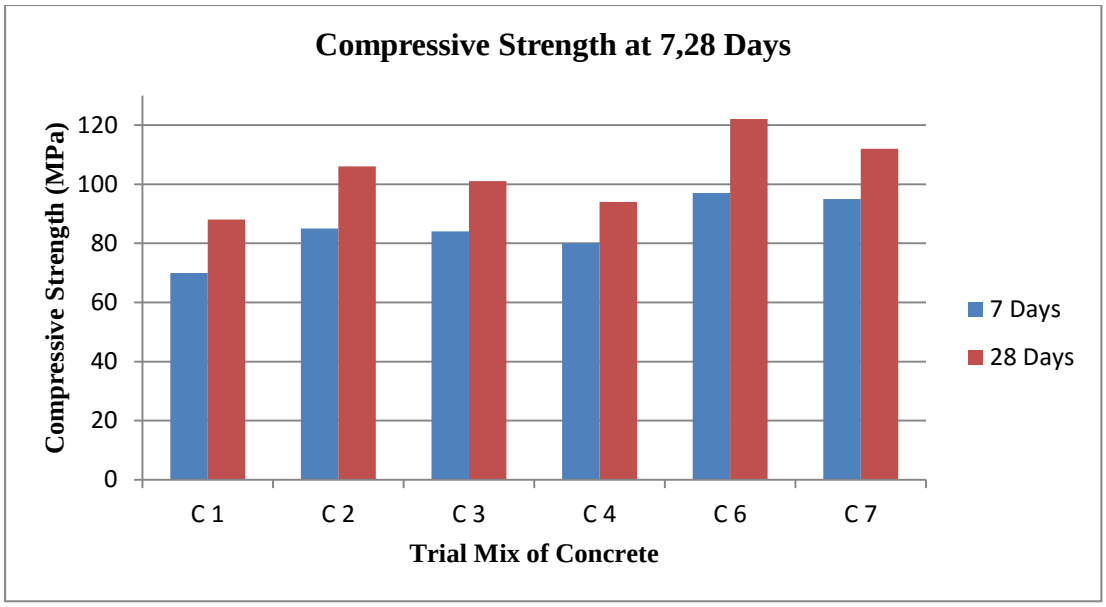

Figure 4. 2 Compressive Strength of 7 days and 28 days of UHP-HFRC Concrete Mix

Table 4. 1 Compressive Strength and Maximum Load of Mortar and Concrete

Property	UHP-HFRC (mortar)		UHP-HFRC (concrete)	
	7 days	28 days	7 days	28 days
Average Maximum Load (kN)	870	1090	975	1220
Compressive strength (MPa)	87	109	97	122

4.3 Comparison of Trial Mix

During this course, 13 trials are done in which 6 trials are of mortar and 7 trials are of concrete. There is variation of nano silica, steel fiber aspect ratio, super plasticizer, and water binder ratio. During the study of trial mix, compressive strength and workability are the two important parameters to fix the mix proportions of UHP-HFRC.

In trial mix M3 and M4, there is variation of nano silica content i.e. in mix M3, nano silica content is zero and in mix M4, the nano silica content is 2% of binder content. As seen in the table 3.13 there is 3% increase in compressive strength of concrete and also nano silica is a liquid content it can also increase some workability of content.

In trial mix, M1, M2 and M3 there is variation of water binder ratio. As we decreases the water content the compressive strength of the mortar increases and workability reduces. As the water content reduces, the voids which were filled with water will be filler material which will increase the strength of mortar i.e. increases from 72MPa to 92MPa. The figure 4.3 shows an effect of water binder ratio on the compressive strength.

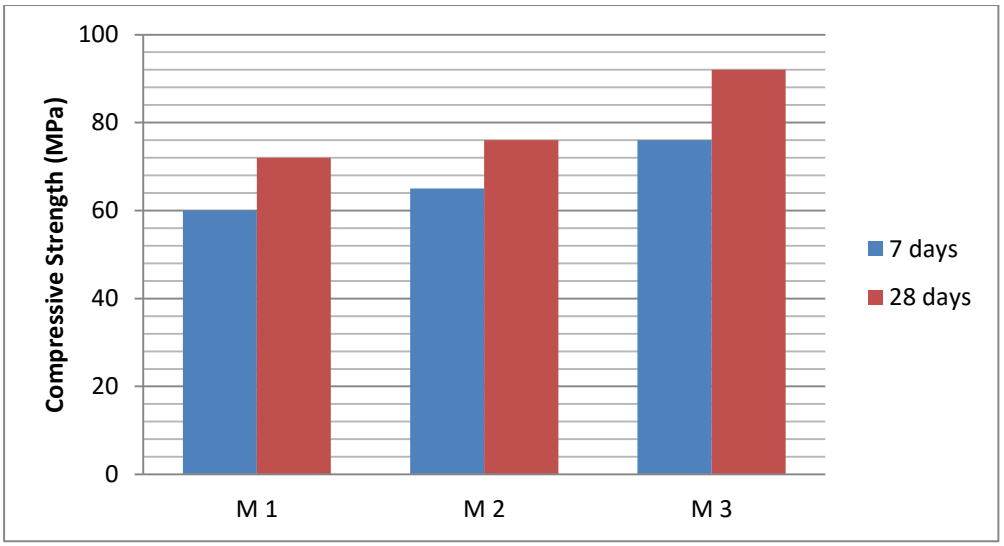

Figure 4. 3 Variation of W/B v/s Compressive Strength

In trial mix C1 and C2, there is variation of aspect ratio of steel fibers i.e. crimped fiber aspect ratio changes from 45 to 25 and the aspect ratio of hooked fiber changes from 85 to 80. As the aspect ratio decreases, there is 15 to 20% increase in compressive strength of concrete.

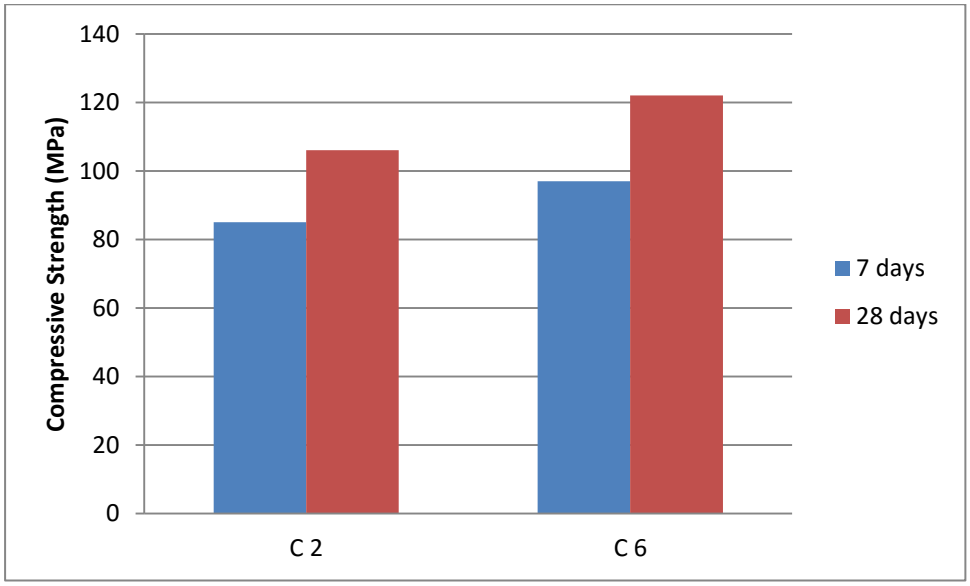

Figure 4. 4 Variation of Steel Fiber v/s Compressive Strength

4.4 Beam Column Joint Testing

In this section, testing of BCJ can be started. Firstly check the damage index of the BCJ. Then check the maximum displacement of the beam column joint by applying cyclic load on beam column so that it can come under ultimate stress and to know about the point where the reinforcement can break.

In my research, when the beam column joint was tested under cyclic loading, the reinforcement broke above 35mm displacement. This shows that in Park and Ang index model, ultimate displacement (δ_u) taken as 35mm. Park and Ang index model is:-

$$D = \frac{\delta_m}{\delta_u} + \frac{\beta}{\delta_u F_y} \int dE$$

In this $\delta_u$is the ultimate displacement and $\delta_m$is the maximum displacement considered.β is the strength degradation parameter whose value is 0.1. F_y is the value of yield strength of structure whose value is calculated from the load displacement hysteresis graph. The theoretical range of damage index for slightly damage is 0.2-0.4, for moderate is 0.4-0.6, for severe is 0.6-0.8 and for complete damage is 1. Calculation of damage index is showed in chapter 3. The other six specimens are tested at different damage index level.

4.4.1 Load hysteresis graph

A. Control specimen

In this section, the hysteresis graphs of BCJ joint are discussed. The graphs are between the load and displacement and indicate about the cyclic behavior of BCJ. Through the graphs, the energy dissipation, stiffness, ductility ratio and strength degradation were calculated. The graph indicates about the load carrying capacity of BCJ and the ultimate displacement it can take.

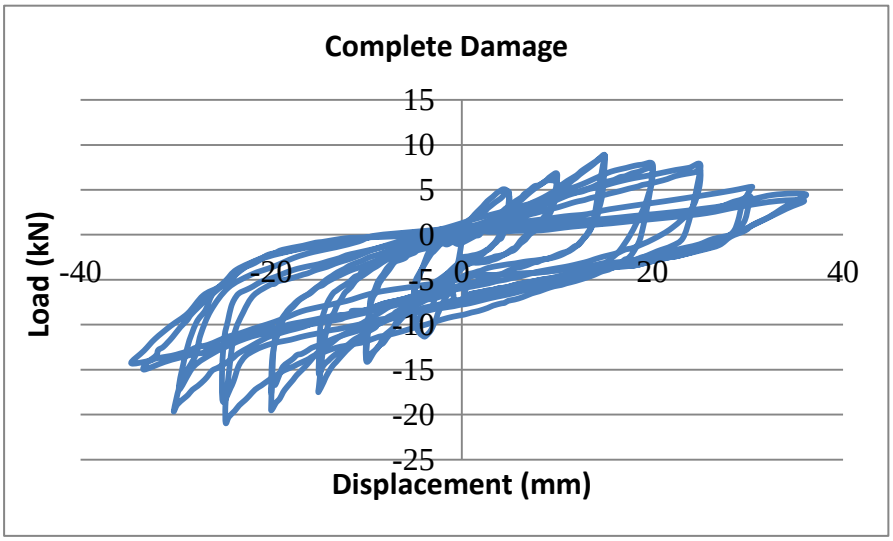

Figure 4. 5 Hysteresis Graph of Complete Damage

From figure 4.5,it can be seen that the cycle peak load starts decreasing from lateral displacement of 25mm for the negative direction i.e. pull and lateral displacement of 15mm for the positive direction i.e. (push). There is sudden drop in the load after 30mm displacement in positive direction. This indicates that yielding of the reinforcement and failure

will occur at 35mm in positive direction. The bond degradation occurs on the compression side of BCJ because the reinforcement on the tension side is 3 bars of 10mm and 2 bars of 8mm on compression side of BCJ.

In figure 4.5, the maximum load achieved by the BCJ on positive displacement side is 8.32kN at 15mm cycle and on negative displacement side the maximum load is 20.2572kN at 25mm. The cracks at the joint go diagonally in the control specimen. The ultimate load achieved by BCJ on positive side is 4.5kN at 35mm and on negative displacement side is 15kN at 35mm.

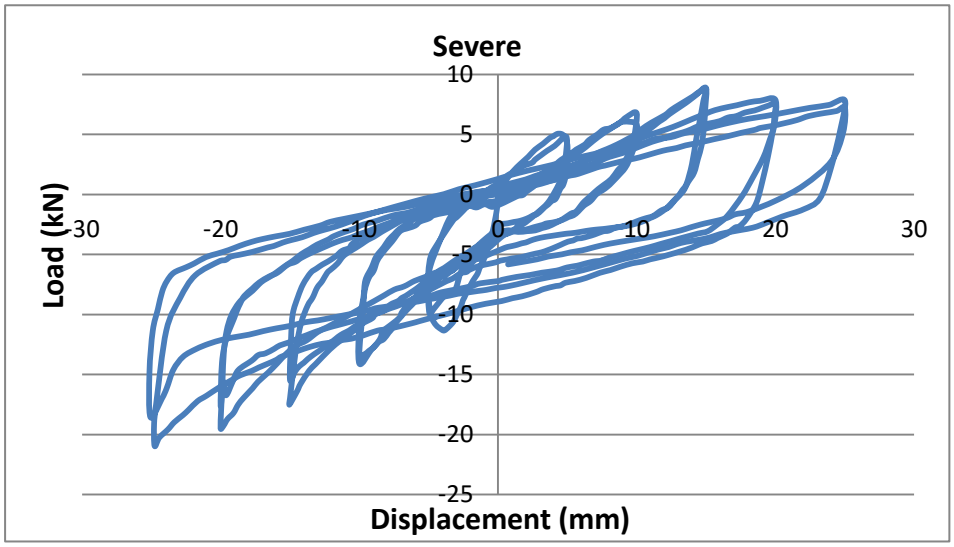

Figure 4. 6 Hysteresis Graph of Severe Damage

In figure 4.6, the maximum load achieved by the BCJ on positive displacement side is 8.32kN at 15mm cycle and on negative displacement side the maximum load is 20.2572kN. The ultimate load achieved by BCJ on positive displacement side is 7.82kN at 25mm and on negative displacement side is 20.25kN at 25mm.

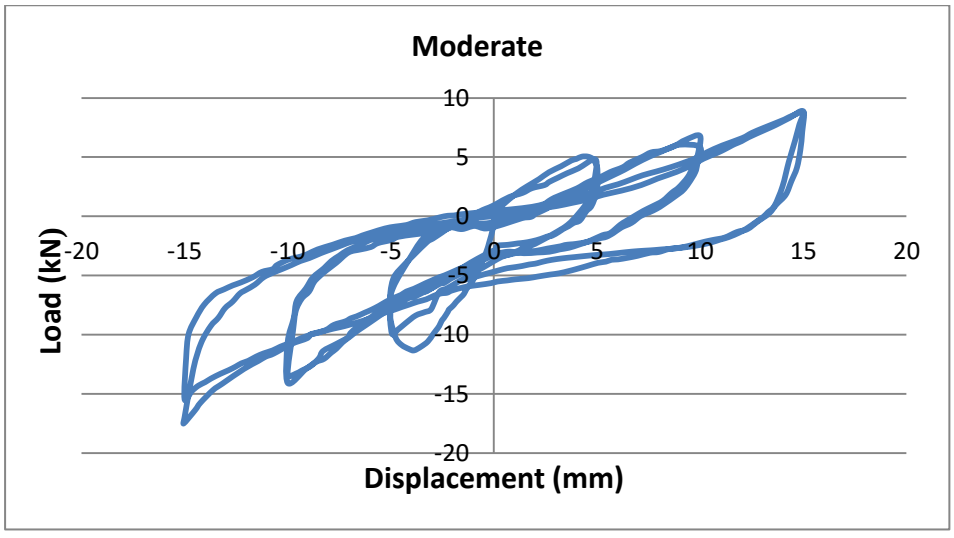

Figure 4. 7 Hysteresis Graph of Moderate Damage

In figure 4.7, the maximum and ultimate load achieved by the BCJ on positive displacement side is 8.32kN at 15mm cycle and on negative displacement side is 20.2572kN at 15mm.

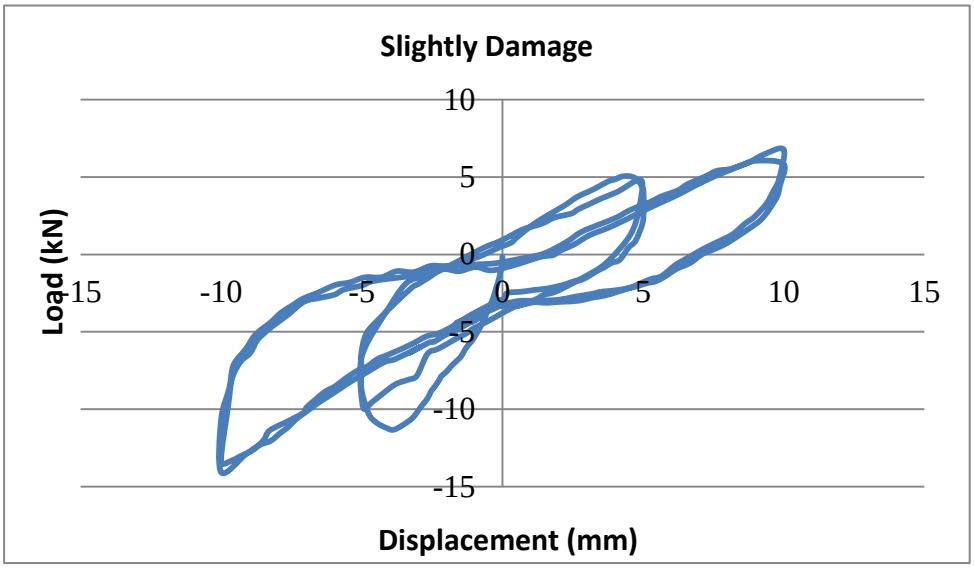

Figure 4. 8 Hysteresis Graph of Slightly Damage

In figure 4.8, the maximum and ultimate load achieved by the BCJ on positive displacement side is 6.77kN at 10mm cycle and on negative displacement side is 14.07kN at 10mm.

B. Retrofitted specimen

The graph tells about the retrofitted behavior of BCJ i.e. shows load carrying capacity of BCJ at different damage level. As the displacement increases, the load increase upto some extent then decreases.

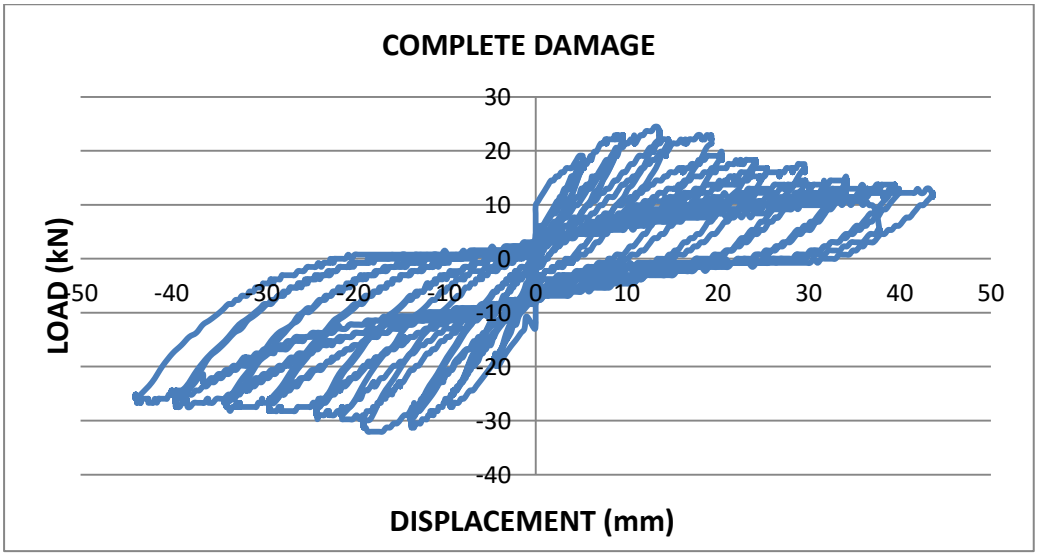

Figure 4. 9 Hysteresis Graph of Retrofitted Specimen at Complete Damage Level

In figure 4.9, the load of R-CD specimen increases on positive side of graph to 10mm and on negative side of graph to 15mm. The maximum load achieved by BCJ on positive

displacement side is 19.448kN and on negative side is 25.934kN. The ultimate load achieved on positive displacement side is 12.2kN and on negative displacement side is 25.94kN. The BCJ failure point is at 45mm where the steel reinforcement yields in the second cycle.

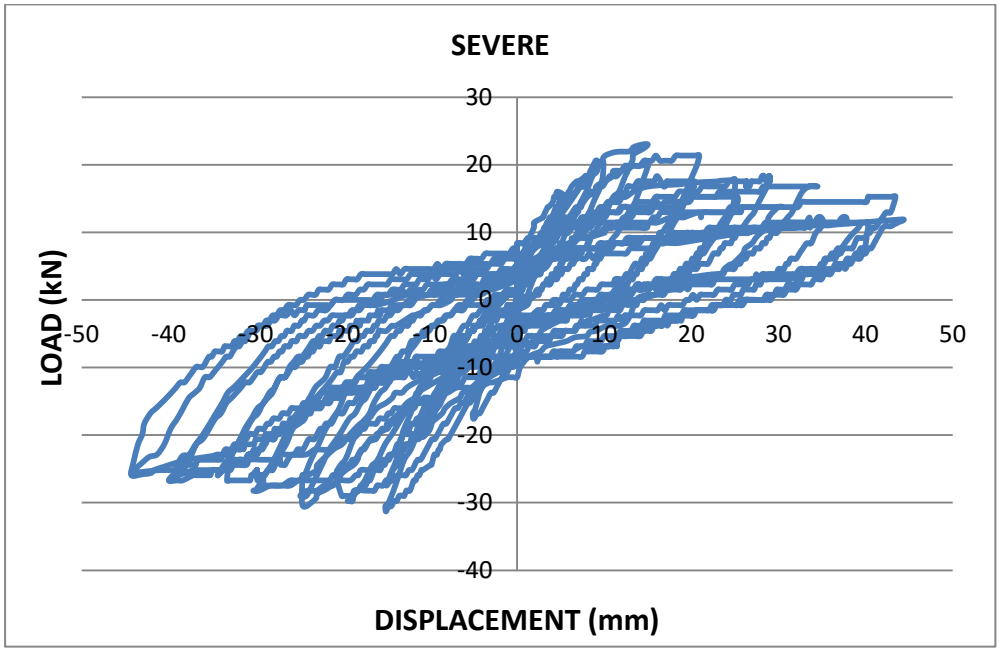

Figure 4. Hysteresis Graph of Retrofitted Specimen at Severe Damage Level

In figure 4.10, the maximum load of R-SED specimen achieved by BCJ on positive displacement side is 21.98kN and on negative displacement side is 29.74kN. The ultimate load achieved on positive displacement side is 15.75kN and on negative displacement side is 25.63kN. The BCJ failure point is 45mm where the steel reinforcement yields in the second cycle.

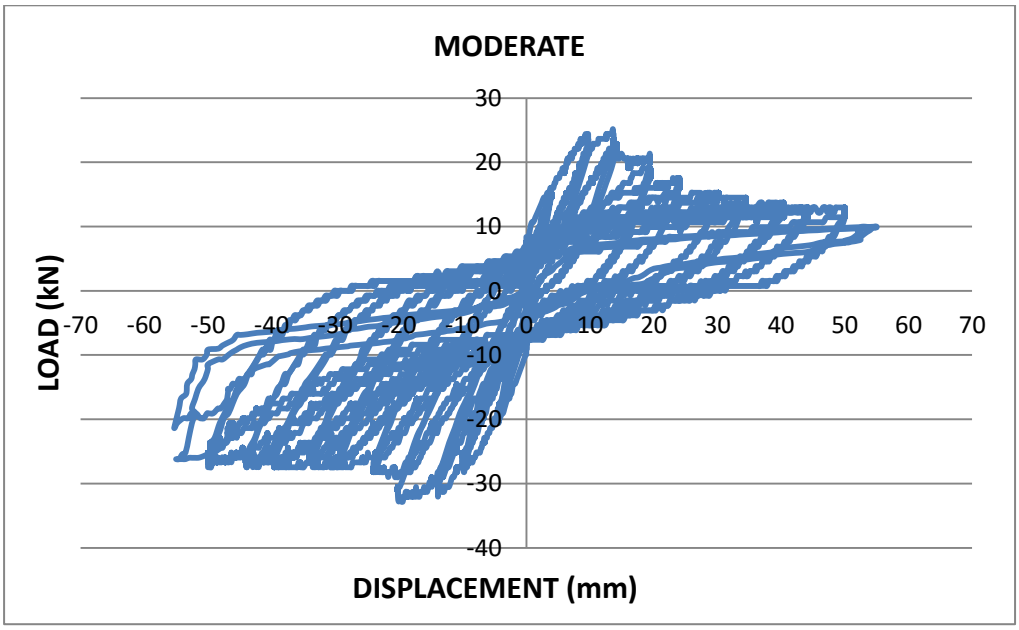

Figure 4. 10 Hysteresis Graph of Retrofitted Specimen at Moderate Damage Level

In figure 4.11, the load of R-MD increases on compression side upto 10mm and on tension side upto 20mm. The maximum load achieved by R-MD beam column joint on compression side is 22.88kN and on tension side is 31.281kN. The BCJ steel reinforcement yields at 55mm.

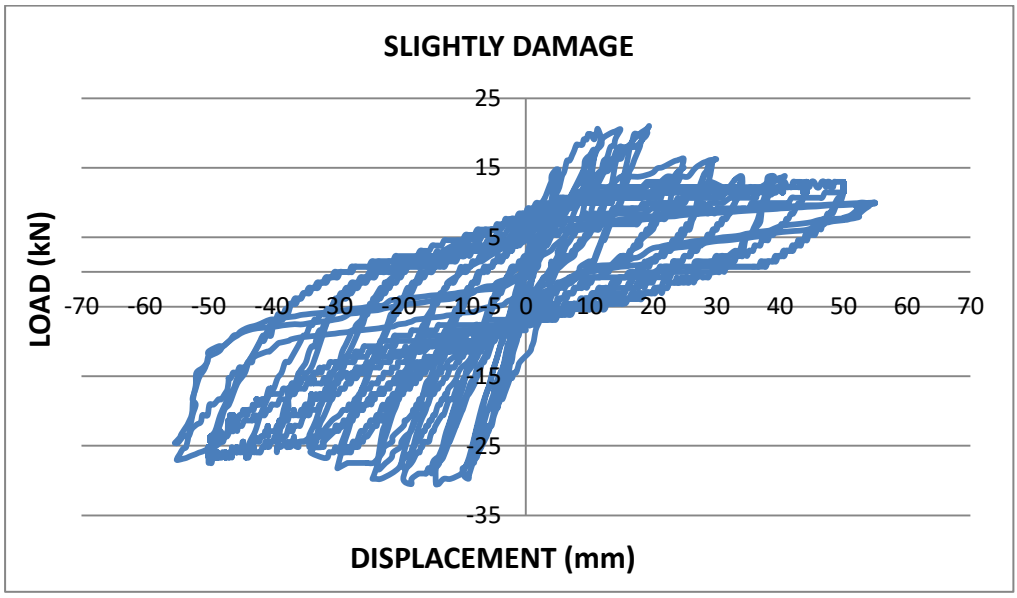

Figure 4. 11 Hysteresis Graph of Retrofitted Specimen at Slightly Damage Level

In figure 4.12, the load of R-SD increases on compression side upto 15mm and on tension side upto 20mm. The maximum load achieved by R-SD beam column joint on compression side is 20.09kN and on tension side is 29.63kN. The BCJ steel reinforcement yields at 55mm.

4.4.2 Ductility Behavior of BCJ

The ductility of the specimen can be calculated from load displacement envelope curve. Firstly make the S- curve envelope to calculate the displacement ductility. The procedure of calculating the displacement ductility as shown in figure 4.13. The formula to calculate the displacement ductility is:-

$$\mu = \frac{(\delta_{u1} + \delta_{u2})}{(\delta_{y1} + \delta_{y2})}$$

Where μ is the ductility displacement, δ_{u1} and $\delta_{u2}$are the ultimate displacement, $\delta_{y1}$and δ_{y2} are the yield displacement.

The comparison of ductility of specimens i.e. R-SD, R-MD, R-SED and R-CD is improved by 17.05%, 17.64%, 31.47% and 32.9% respectively as compared with C-CD. The efficiency of UHP-HFRC sustain the load in post elastic region as compared to initial damage of retrofitted specimen. It is shifted from complete damage to slightly damage.

During testing, it was observed that before retrofitting, the cracks at the joint region of BCJ goes diagonally in the column and after the retrofitting, the crack will be at the joint only.

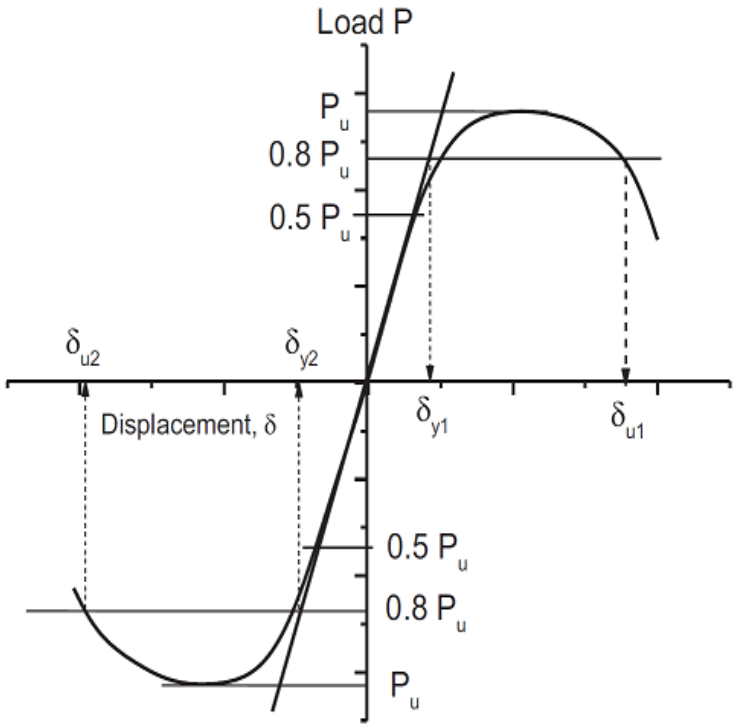

Figure 4. 12 Procedure to Calculate Ductility (Raju et al.2019)

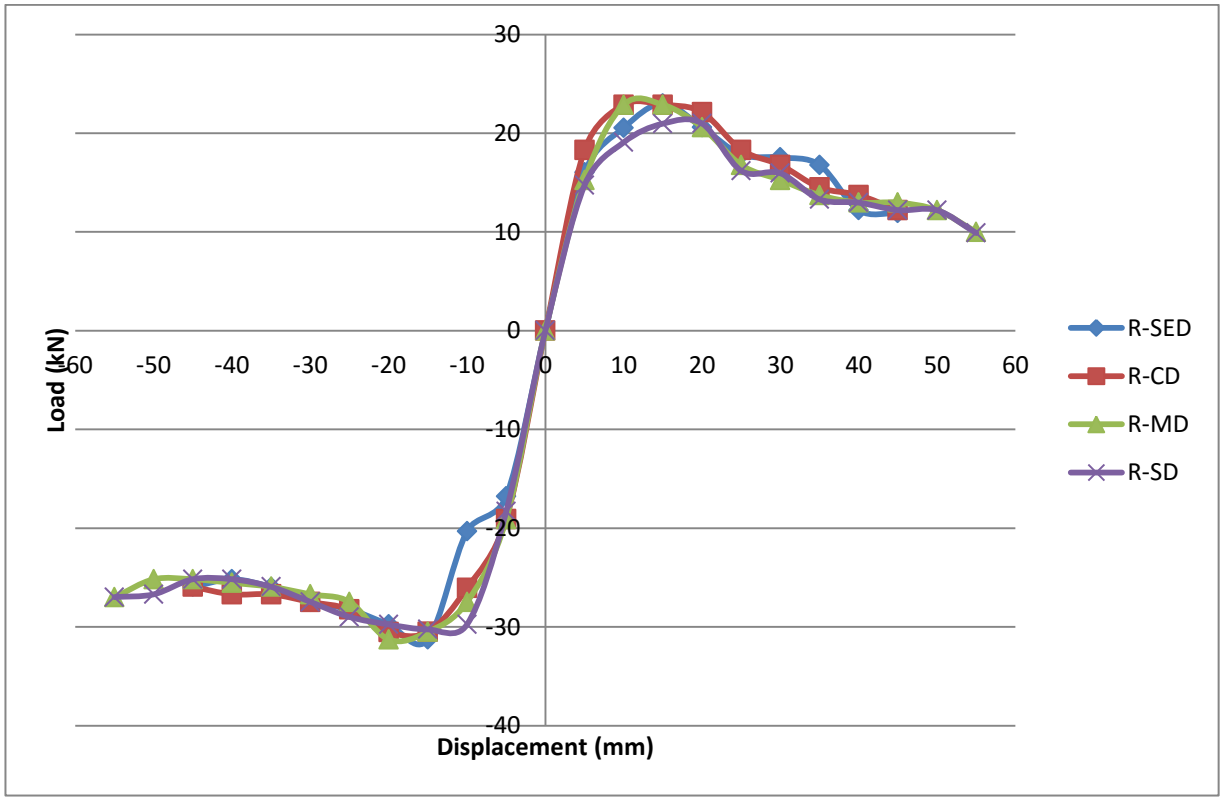

Figure 4. 13 S Curve of Retrofitted Specimen

Table 4. 2 Calculation of Displacement Ductility

Specimen	Maximum				Ultimate				Displacement		
	Positive		Negative		Positive		Negative				
	Pm max (kN)	Dm (mm)	Pm max (kN)	Dm (mm)	Pm max (kN)	Dm (mm)	Pm max (kN)	Dm (mm)	Yield (D)	Ultimate (D)	Ductility UD/YD
C-CD	8.83	15	19.74	25	4.14	35	14.6	35	17.4	59.2	3.40
R-CD	19.448	10	25.934	15	10.37	45	22.09	45	16.2	64.5	3.98
R-SED	23.0125	15	31.29	15	11.9	45	25.94	45	17	68	4
R-MD	22.88	10	31.281	20	9.99	55	27	55	18	80.6	4.46
R-SD	20.98	20	30.25	15	9.89	55	26.98	55	14.8	67	4.53

4.4.3 Stiffness and Strength Degradation

The stiffness is also defined as the ratio between the load and displacement. The slope of line joining the peak point on the negative and the positive direction of a hysteresis loop is called peak to peak stiffness. The percentage change in the load between the two adjacent curves of hysteresis loop is called strength degradation.

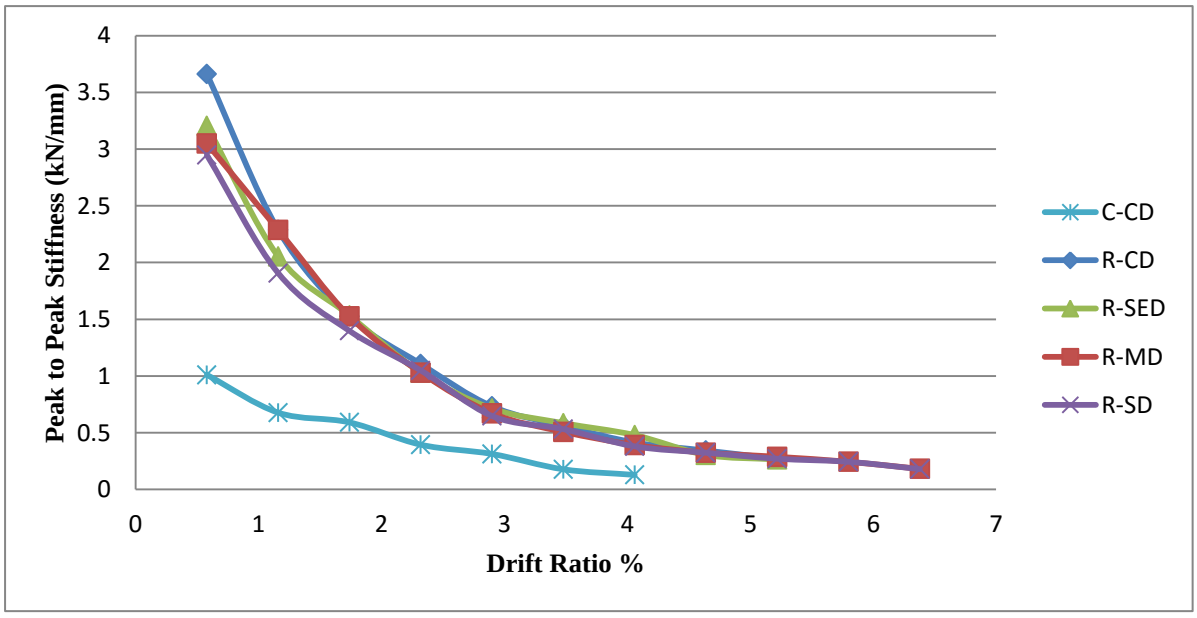

Figure 4. 14 Peak to Peak Stiffness v/s Drift Ratio

In figure 4.14, as the number of cycle increases, the stiffness of the BCJ decreases. In C-CD specimen, the stiffness is 0.9598 kN/mm at 0.58 drift ratio. The drift ratio of 35mm cycle of complete damage is 4.06 and the stiffness of BCJ becomes 0.1287 kN/mm.

It can be observed from the figure 4.14 that all the retrofitted specimens using CFRP confined with UHP-HFRC, the stiffness becomes 3 to 3.7 times the control specimen. For initially damaged specimens, the drift ratio at which it loses its stiffness will increase after retrofitting. The lower rate of stiffness degradation was observed from the graph in all retrofitted specimens.

The figure 4.15 and 4.16 show that the graph is between the strength degradation and drift ratio which shows that as drift ratio increases the strength degradation also increases. The strength degradation of tension and compression side is calculated for all retrofitted specimens. The retrofitted specimens using CFRP confined with UHP-HFRC improves the strength degradation at larger value of drift ratio. In graph, the R-SED shows the lowest value on positive drift i.e. 59.58% and R-CD shows the lowest value on negative drift ratio side i.e. 15.82%.

a) Control Specimen

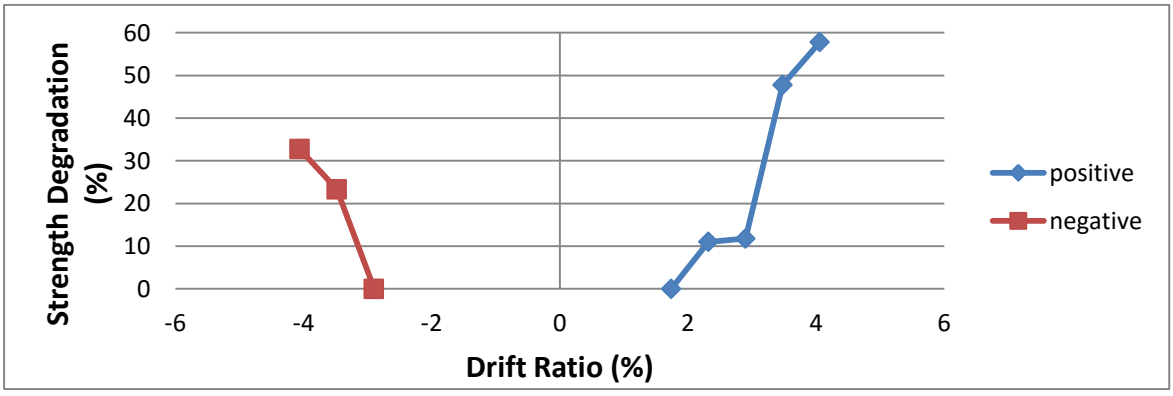

Figure 4. 15 Strength Degradation v/s Drift Ratio of Control Specimen

b) Retrofitted Specimens

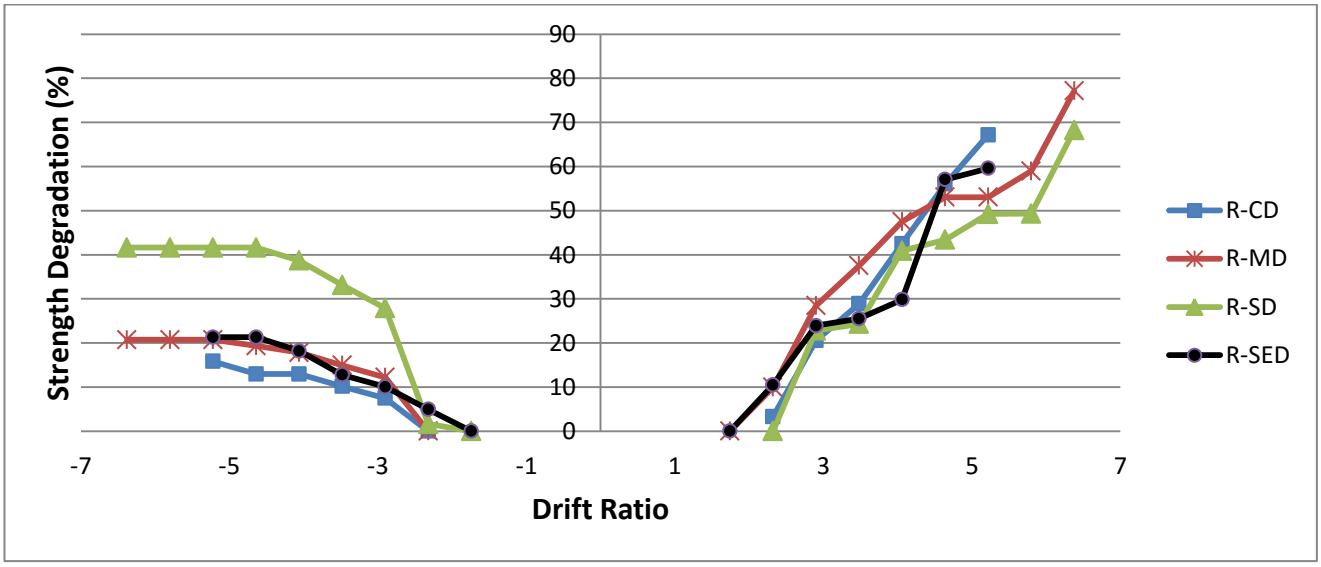

Figure 4. 16 Strength Degradation v/s Drift Ratio of Retrofitted Specimens

4.4.4 Energy Dissipation

The energy dissipation is important parameter of BCJ which tells about the structural response during the earthquake. The energy dissipation is the area enclosed in the load displacement hysteresis loop at different drift ratio. The cumulative energy dissipation and per cycle energy dissipation of all BCJ i.e. C-CD, R-CD, R-SED, R-MD, R-SD specimens are plotted. Under cyclic loading, all the retrofitted specimens dissipate more energy as compared to C-CD specimen. Further, decrease in damage level from R-CD to R-SD, there is increase in ultimate displacement as well as energy dissipation as compared to C-CD specimen. The sequence of retrofitted specimens in terms of energy dissipation is R-CD<R-SED<R-MD<R-SD.

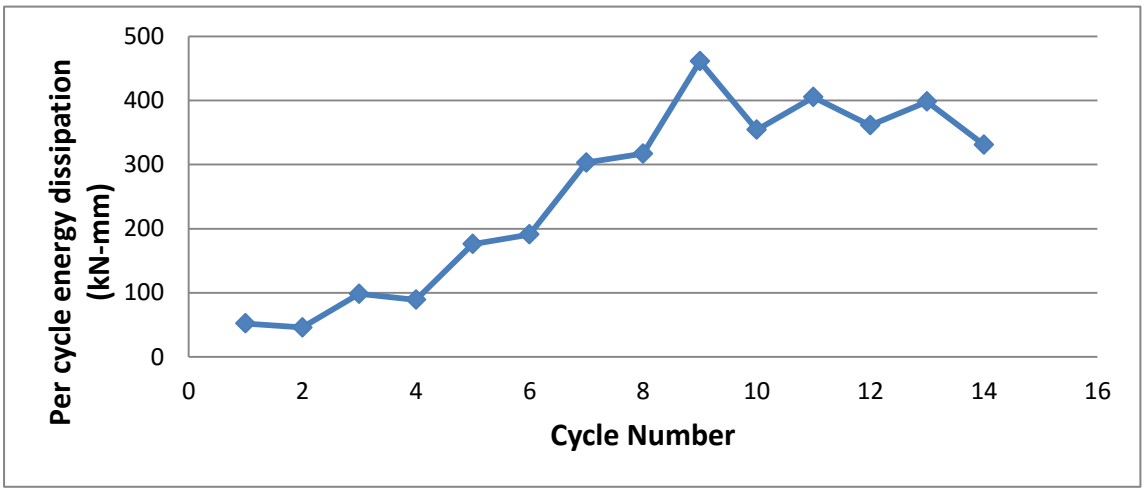

Figure 4. 17 Per Cycle Energy Dissipation v/s Cycle Number of Control Specimen

In figure 4.18, R-SD and R-MD has ability to dissipate the energy at higher drift ratio i.e. it resists the opening of crack at the lower drift ratio due to the hybrid steel fibers used.

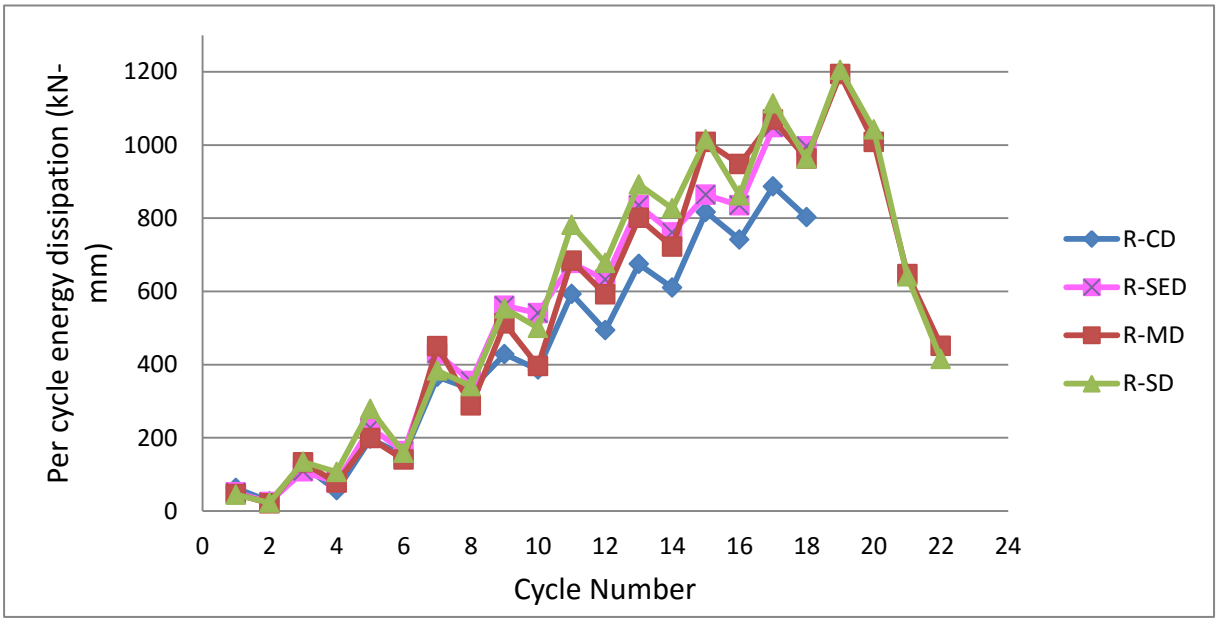

Figure 4. 18 Per Cycle Energy Dissipation v/s Cycle Number of Retrofitted Specimen

As cycles of R-CD specimen increases, the energy dissipation also increases upto 9th cycle i.e. 25mm and after 9th cycle energy dissipation decreases. But in retrofitted specimen, energy dissipation of R-CD and R-SED specimen increases upto 18th cycle. But in case of R-MD and R-SD, the energy dissipation increases upto 19th cycle after that decreases.

The cumulative energy graph describes the behavior of structure for the complete span of earthquake. The C-CD specimen dissipates the energy upto drift ratio of 4.12%, whereas the R-SD, R-MD, R-SED, and R-CD dissipates the energy 56.35%, 56.35%, 28.39% and 28.39% respectively higher than C-CD specimen. In terms of energy dissipation and ductility, the retrofitted specimen gives better performance than control specimen.

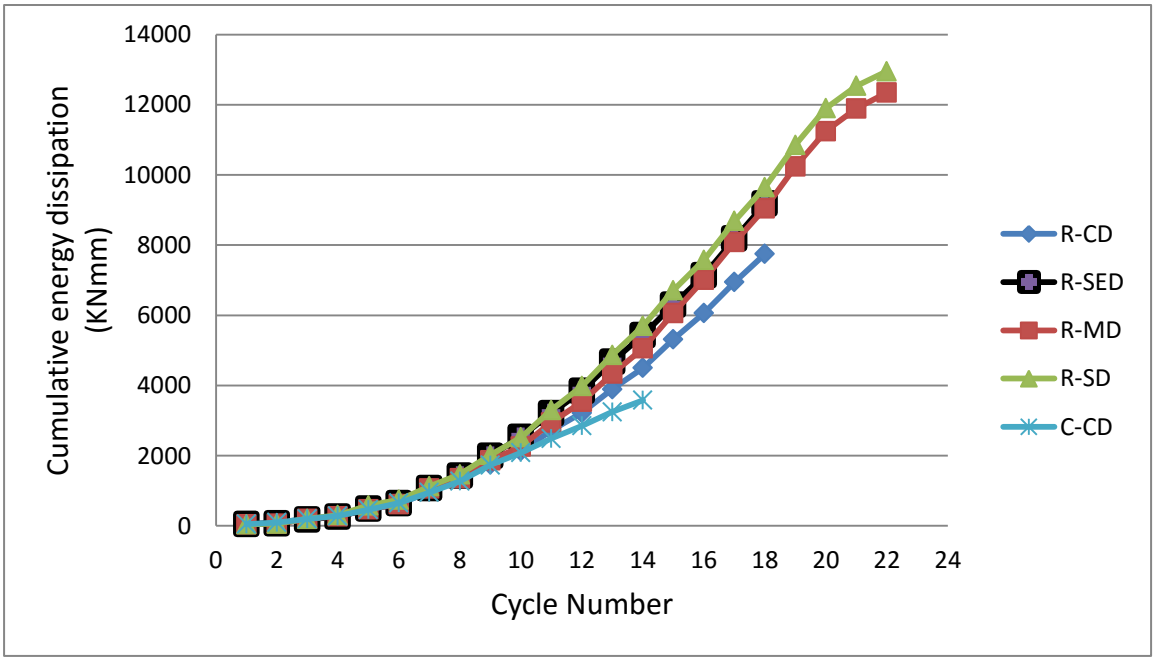

Figure 4. 19 Cumulative Energy Dissipation v/s Cycle Number of Control and Retrofitted Specimen

4.4.5 Moment Rotation

The moment can be calculated by product of peak load of each cycle with the beam length. It is observed from the graph that the moment value on the positive rotation side is less and on the negative rotation side the value of moment is higher.

a) Control Specimen

It is observed from the graph that in C-CD the maximum moment value on positive rotation side is 7.54kNm and on the negative rotation side is 17.8kNm. The ultimate load achieved by the BCJ on positive rotation side is 3.833 kNm at .0406 rotation. On the other side of BCJ is 12.75 kNm at 0.0406 rotation.

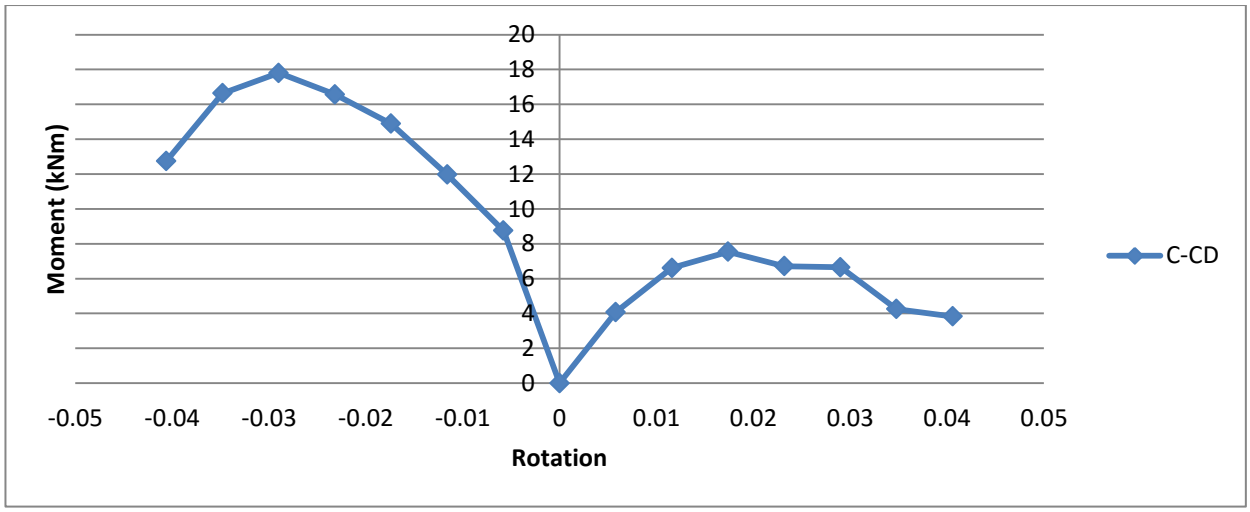

Figure 4. 20 Moment Rotation of Control Specimen

It shows that the moment is higher on the negative rotation side. The moment at the center point is zero shown in figure 4.2 because the beam at that time is at rest and there is no moment.

b) Retrofitted Specimen

In case of R-SD, R-MD, R-SED, and R-CD, the maximum value on positive side is 17.82kN, 19.448kN, 19.48kN and 19.49kN respectively. The moment becomes 2.36, 2.57, 2.58 and 2.584 times higher than C-CD specimen and on the negative side moment is 25.7125kN, 26.58kN, 26.59kN and 25.93kN respectively i.e. the moment of retrofitted specimens becomes 1.44, 1.49, 1.494 and 1.456 times higher than C-CD specimen. This predicts that after retrofitting, moment of the BCJ becomes higher than control specimen.

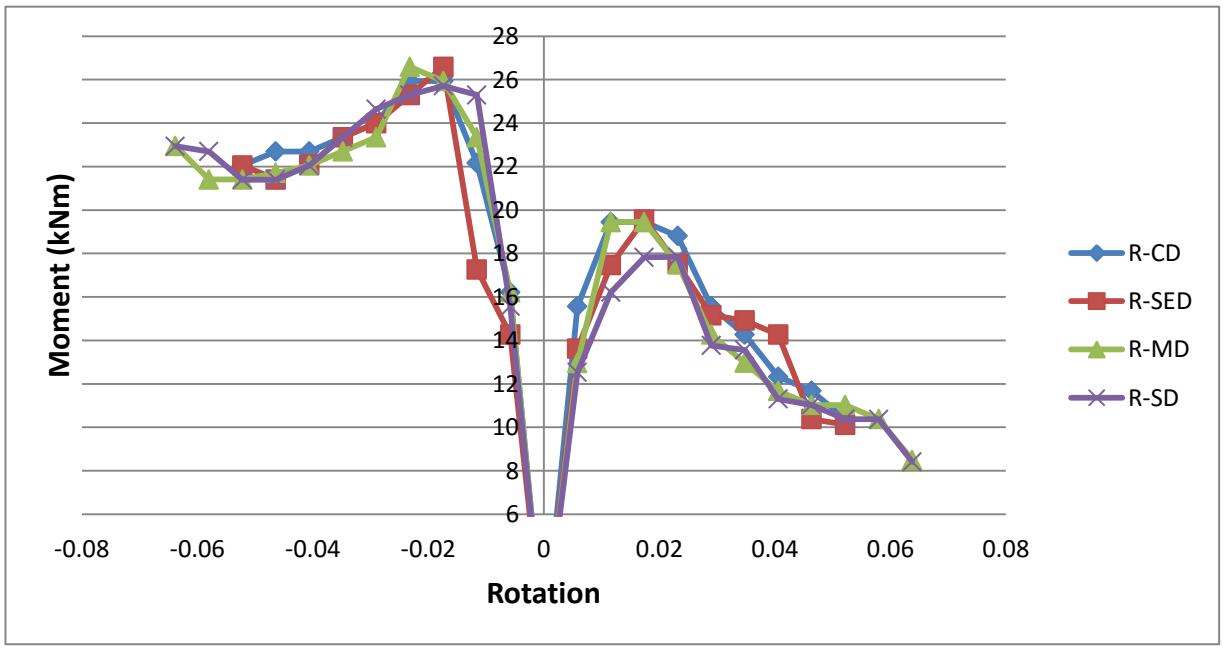

Figure 4. 21 Moment Rotation of Retrofitted Specimen

4.4.6 Joint Principle Tensile Stress

The principle tensile stresses are calculated by using the Priestley equations. The joint principle stresses are calculated for control specimen and all retrofitted specimens.

$$\tau_{jh} = \frac{P}{A}\left(\frac{L_b}{d_b} - \frac{L_b + 0.5D_c}{L_c}\right)$$

$$\sigma_p = (N_c + P)/(b_c h_c)$$

$$\sigma_t = \frac{\sigma_p}{2} + \sqrt{\frac{\sigma_p^2}{4} + {\tau_{jh}}^2}$$

Where P is the applied cyclic load, A is the area of horizontal cross section area, L_b is the length of beam, d_b is the effective depth of beam, L_c is the length of column, D_c is the total depth of beam, N_c is the 10% of axial load carrying capacity of column, b_c is the width of beam.

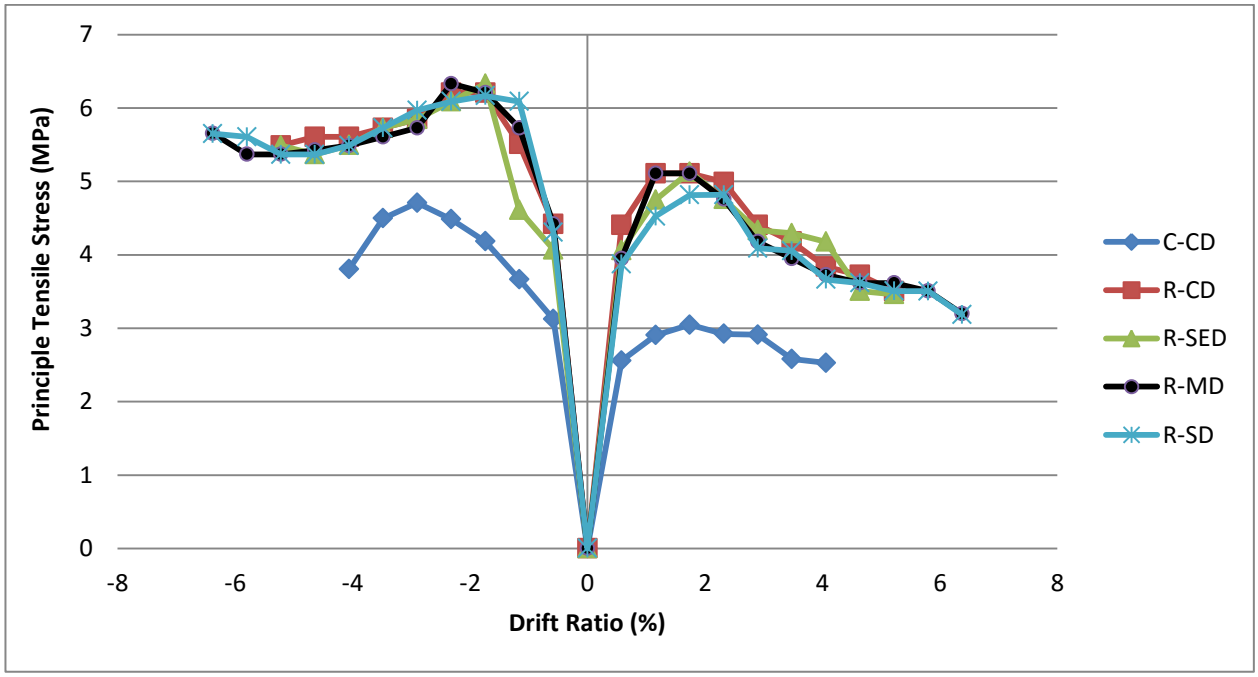

Figure 4. 22 Principle Tensile Stress v/s Drift of Control and Retrofitted Specimen

It is observed from the figure 4.22, that the maximum value of tensile stress of C-CD on the positive drift side is 3.07MPa and on the negative side is 4.71MPa. The maximum value of R-SD, R-MD, R-SED, and R-CD on the positive drift side is 4.81kN, 5.12kN, 5.12kN, 5.18kN respectively and on negative side is 6.16kN, 6.2kN, 6.32kN, 6.21kN respectively. The tensile strength of retrofitted specimen is 1.5 times the value of control specimen All the retrofitted specimens show improvement in the joint principle tensile stress i.e. there is increase in the value of tensile stresses as compared to C-CD specimen. By using the UHP-HFRC and CFRP

increases the tension carrying capacity of the compression face of BCJ and resist the growth of cracks at the joint.

4.4.7 Crack and Failure Analysis

The cracking pattern of retrofitted and control specimen analysis done in this section. The control specimen behaves as brittle in nature at joint as the cracks go in a diagonal way at the joint section whereas retrofitted BCJ behave as ductile in nature and plastic hinge formation takes place at the joint and the BCJ will fail at joint only and cracks will not go to the diagonal section of column. Due to plastic hinge formation, the structure will not collapse as the failure of beam take place only. As the confinement of BCJ using CFRP confined with UHP-HFRC will increase the tensile strength, therefore diagonal cracks are formed at a joint. The concrete spell out in wedge shaped at the joint of C-CD at ultimate drift. The yielding of the reinforcement on the compression face makes the number of cracks on the face. The hair line cracks are formed on the beam but after retrofitting these hair line cracks are very less as compared to control specimen. This shows that UHP-HFRC and CFRP will make the retrofitting better for the seismically designed structures.

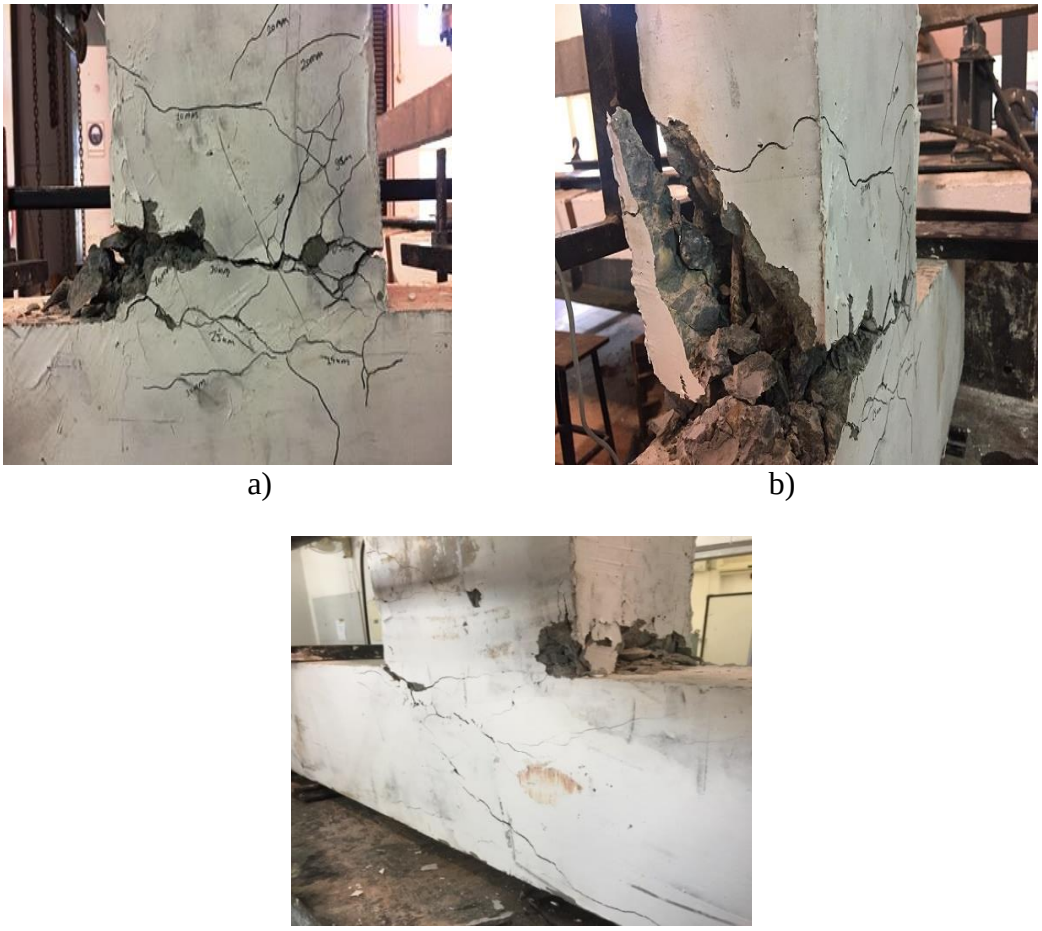

a) b)

c)

Figure 4. 23 Crack and Failure Pattern of Control Specimen

a)

b)

c)

d)

e)

f)

g)

Figure 4. 24 Failure Pattern of a) C-SED, b) C-MD, c) C-SD, d) R-CD, e) R-SED, f) R-MD, g) R-SD

CHAPTER 5

CONCLUSIONS

1) The load hysteresis behavior of retrofitted beam column joint significantly improved as compared to control specimen. The hybrid fibers in UHP-HFRC and CFRP impart the confinement and provide the ductile plateau in a post-elastic stage of the retrofitted specimen.
2) The load deformation envelope indicates the improvement in the ductility of all initially damaged retrofitted BCJ. The ductility of R-SD, R- MD, R-SED, and R-CD is improved by 17.05%, 17.64%, 31.47% and 32.9% respectively as compared to C-CD.
3) The peak to peak stiffness of all the retrofitted BCJ is higher than C-CD specimen. The R-SD and R-MD specimen enable to perform better at a higher drift ratio than R-CD. The peak to peak lateral stiffness performance of all retrofitted specimens at the ultimate drift can be R-SD > R- MD > R-SED > R-CD.
4) The energy dissipation affects by intial damage of specimen ata very higher drift. C-CD specimen dissipates the energy upto 4.12%, whereas the R-SD, R-MD, R-SED, and R-CD dissipates the energy 56.35%, 56.35%, 28.39% and 28.39% respectively higher than C-CD specimen. Hence, this retrofitting technique is favorable for complete, severe, moderate and slight damaged structure elements, and these retrofitted elements always provide better results under strong ground motion.
5) The joint principal tensile stress carrying capacity of the retrofitted specimen increases as compared to C-CD specimen. However, as the initial damage level increases the principal tensile stress capacity of R-SD, R-MD, and R-SED in negative drift increases as compared to positve drift. The lack of residual strength in compression face reinforcement exhausts sooner and thereafter, higher stresses transferred on CFRP and then hybrid fiber-matrix bond which led to failing the joint to hold the principal tensile stress for higher drift.

REFERENCES

ACI Committee 318 (2014) Building Code Requirements for Structural Concrete, American Concrete Institute.

Bansal, P. P., Kumar, M. and Dar, M. A. (2016) 'Retrofitting of exterior RC beam-column joints using ferrocement jackets', Earthquake and Structures, 10(2), pp. 313–328. doi: 10.12989/eas.2016.10.2.313.

Beschi, C. et al. (2015) 'HPFRC Jacketing of non seismically detailed RC corner joints', Journal of Earthquake Engineering, 19(1), pp. 25–47. doi: 10.1080/13632469.2014.948646.

Bonacci, J. F. and Leon, R. T. (1976) 'Recommendations for Design of Beam-Column Joints in Monolithic Reinforced Concrete Structures', ACI Journal Proceedings, 73(7), pp. 1–37. doi: 10.14359/11078.

BUREAU OF INDIAN STANDARDS (2004) 'IS 516 -1959: Method of Tests for Strength of Concrete', IS 516 -1959: Method of Tests for Strength of Concrete.

Cement, O. P. (2013) 'Bureau of Indian Standard (BIS). Ordinary Portland Cement 53 grade - Specifications:IS12269', (March).

Committee, A. C. I. (2014) ACI 318R-14.

Hoang, A. Le et al. (2019) 'Experimental study on structural performance of UHPC and UHPFRC columns confined with steel tube', Engineering Structures. Elsevier, 187(January), pp. 457–477. doi: 10.1016/j.engstruct.2019.02.063.

IS-4031 (Part V) (1988) 'Methods of Physical Tests for Hydraulic Cement-Determination of Initial and Final Setting Times', Bureau of Indian Standards, New Delhi.

IS:13920-1993 (1993) 'Ductile Detailing of Reinforced Concrete Structures Subjected To Seismic Forces -Code of Practice', Bureau of Indian Standards, New Delhi.

IS:2386 (Part lll) (1963) 'Method of Test for aggregate for concrete.', Bureau of Indian Standards, New Delhi, p. (Reaffirmed 2002).

IS 10262 (2009) 'Guidelines for concrete mix design proportioning', Bureau of Indian Standards,New Delhi, pp. 1–21.

IS 4031(Part 6), I. S. (2005) ‘Indian Standard Is: 4031 (Part 6) - 1988 (Reaffirmed 2005). Methods Of Physical Tests For Hydraulic Cement Part 6 Determination Of Compressive Strength Of Hydraulic Cement Other Than Masonry Cement (First Revision)’, Bureau of Indian Standards,New Delhi, pp. 1–3. Available at: https://ia800400.us.archive.org/0/items/gov.in.is.4031.6.1988/is.4031.6.1988.

IS 650: (1991). Specification for Standard Sand for Testing of Cement.

IS 383: (1970). Specification for Coarse and Fine Aggregates From Natural Sources For Concrete.

(IS 10262, 2009)— (2002) ‘Indian Standard CRITERIA FOR EARTHQUAKE RESISTANT DESIGN OF STRUCTURES BUREAU OF INDIAN STANDARDS’, Is, 1893(1). Available at: http://rahat.up.nic.in/sdmplan/Earthquake/AnnexureI-V/AnnexureI_Bldg. Earthquake.

Kisan, M. et al. (1988) ‘IS 4031 Part 11, Mthod of physical tests for hydraulic cement, Part 11: Determination of density [CED 2: Cement and Concrete]’, Indian Standard, pp. 2–6.

Köksal, F. et al. (2008) ‘Combined effect of silica fume and steel fiber on the mechanical properties of high strength concretes’, Construction and Building Materials, 22(8), pp. 1874–1880. doi: 10.1016/j.conbuildmat.2007.04.017.

Kou, S. C., Poon, C. S., & Agrela, F. (2011). Comparisons of natural and recycled aggregate concretes prepared with the addition of different mineral admixtures. Cement and Concrete Composites, 33(8), 788-795.

Le-Trung, K. et al. (2010) ‘Experimental study of RC beam-column joints strengthened using CFRP composites’, Composites Part B: Engineering. Elsevier Ltd, 41(1), pp. 76–85. doi: 10.1016/j.compositesb.2009.06.005.

Lee, W. T., Chiou, Y. J. and Shih, M. H. (2010) ‘Reinforced concrete beam-column joint strengthened with carbon fiber reinforced polymer’, Composite Structures. Elsevier Ltd, 92(1), pp. 48–60. doi: 10.1016/j.compstruct.2009.06.011.

Mazloom, M., Ramezanianpour, A. A. and Brooks, J. J. (2004) ‘Effect of silica fume on mechanical properties of high-strength concrete’, Cement and Concrete Composites, 26(4), pp. 347–357. doi: 10.1016/S0958-9465(03)00017-9.

Parra-Montesinos, G. J., Peterfreund, S. W. and Chao, S. H. (2005) 'Highly damage-tolerant beam-column joints through use of high-performance fiber-reinforced cement composites', ACI Structural Journal, 102(3), pp. 487–495.

Rajagopal, S. and Prabavathy, S. (2015) 'Investigation on the seismic behavior of exterior beam–column joint using T-type mechanical anchorage with hair-clip bar', Journal of King Saud University - Engineering Sciences. King Saud University, 27(2), pp. 142–152. doi: 10.1016/j.jksues.2013.09.002.

Saghafi, M. hossein and Shariatmadar, H. (2018) 'Enhancement of seismic performance of beam-column joint connections using high performance fiber reinforced cementitious composites', Construction and Building Materials. Elsevier Ltd, 180, pp. 665–680. doi: 10.1016/j.conbuildmat.2018.05.221.

Shaaban, I. G. and Seoud, O. A. (2018) 'Experimental behavior of full-scale exterior beam-column space joints retrofitted by ferrocement layers under cyclic loading', Case Studies in Construction Materials. Elsevier, 8(September 2017), pp. 61–78. doi: 10.1016/j.cscm.2017.11.002.

Sharma, R. and Bansal, P. P. (2019) 'Behavior of RC exterior beam column joint retrofitted using UHP-HFRC', Construction and Building Materials. Elsevier Ltd, 195, pp. 376–389. doi: 10.1016/j.conbuildmat.2018.11.052.

Singh, V. et al. (2014) 'Experimental studies on strength and ductility of CFRP jacketed reinforced concrete beam-column joints', Construction and Building Materials. Elsevier Ltd, 55, pp. 194–201. doi: 10.1016/j.conbuildmat.2014.01.047.

Su, Y., Wu, C., Li, J., Li, Z. X., & Li, W. (2017). Development of novel ultra-high performance concrete: From material to structure. *Construction and Building Materials*, *135*, 517-528.

Yardımcı, M. Y., Aydın, S., & Karabulut, A. Ş. (2009). Mechanical properties of reactive powder concrete containing mineral admixtures under different curing regimes. Construction and building materials, 23(3), 1223-1231

Yu, R., Spiesz, P. and Brouwers, H. J. H. (2014) 'Cement and Concrete Research Mix design and properties assessment of Ultra-High Performance Fibre Reinforced Concrete (UHPFRC)', 56, pp. 29–39. doi: 10.1016/j.cemconres.2013.11.002.